

ETH Zurich - Departement of Earth Sciences

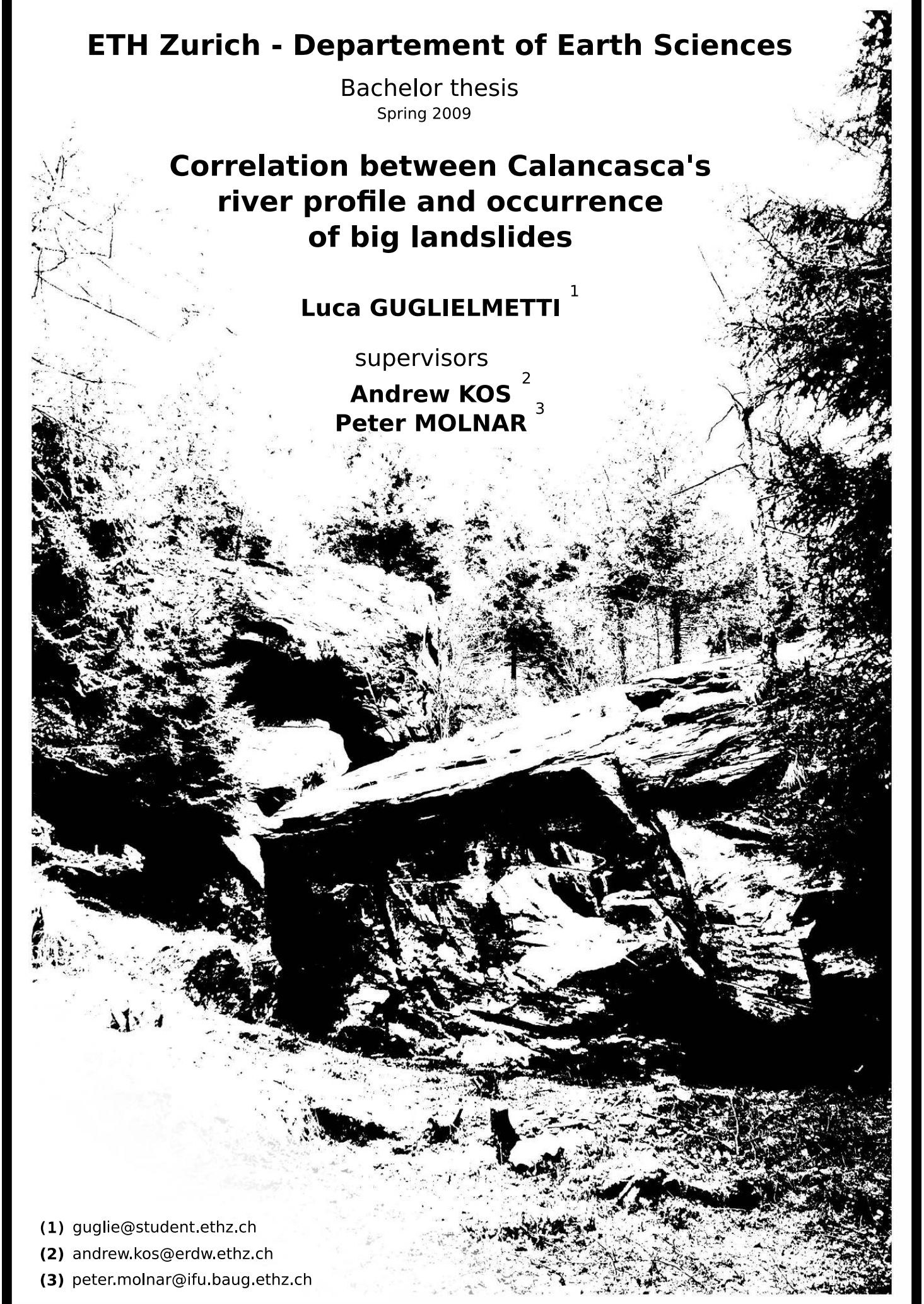
Bachelor thesis
Spring 2009

**Correlation between Calancasca's
river profile and occurrence
of big landslides**

Luca GUGLIELMETTI¹

supervisors

Andrew KOS²
Peter MOLNAR³

- 
- (1) guglie@student.ethz.ch
(2) andrew.kos@erdw.ethz.ch
(3) peter.molnar@ifu.baug.ethz.ch

Alle streghe di ieri e di oggi.

Come streghe venivano considerate tutte quelle persone di bassa condizione,
d'intelligenza singolare che cercavano di distinguersi e di introdurre idee nuove [...]
[Bertossa, 1937]

Contents

1	Introduction	5
1.1	Previous work	5
1.2	Study area overview	5
1.3	Research objectives	5
2	Data	7
2.1	Digital models	7
2.2	Streamflow	7
2.3	Field observation	8
2.4	Cartographic material	8
3	Methods	9
3.1	River profiles	9
3.1.1	Long river profile	9
3.1.2	Cross sections	11
3.2	Geological analysis	11
3.2.1	Sedimentology of the river bed	11
3.2.2	Morphology	12
3.3	Hydrological analysis	13
3.3.1	Periodicity	13
3.3.2	Probability	13
3.3.3	Extreme event analysis	14
3.4	Hydrological modeling	15
3.4.1	Backwater-curve's algorithm	15
3.4.2	Sediment motion	17
4	Results	18
4.1	Geological results	18
4.1.1	Sedimentology of the river bed	18
4.1.2	Long river profile	22
4.1.3	Morphology	24
4.1.4	Cross sections	24
4.2	Hydrological results	28
4.2.1	Periodicity	28
4.2.2	Empirical streamflow-trend	28
4.2.3	Flood analysis	28
4.2.4	Sediment motion	29
4.2.5	Backwater-curve simulation	33

5	Interpretations	37
5.1	Quality of the digital models	37
5.2	First interpretation	37
5.3	Second interpretation	38
6	Conclusions	39
6.1	Summary	39
6.2	Future work	39
6.3	Acknowledges and thanks	40
A	Additional data	43
A.1	Additional tables	43
A.2	Additional maps	44
B	Source codes	50
B.1	Backwater curve simulation	50
	B.1.1 main.m	50
	B.1.2 get_area.m	54
	B.1.3 get_perimeter.m	54
B.2	Additional codes	55
	B.2.1 Smaller Matlab programs	55
	B.2.2 L ^A T _E Xsource files	55

Chapter 1

Introduction

1.1 Previous work

In Switzerland there are more than 50 large ($> 1 \text{ km}^2$) rock-slope failures listed in the Swiss Alps [Abele, 1974] and many more were detected later [Eisbacher and Clague, 1984].

It is known that large landslides and rockfalls can influence the development of stream dynamics and valley morphology in confined alpine valleys. In particular Korup analysed many rivers of Switzerland and New Zealand and showed that landslide and rock fall debris that become deposited in the stream bed have the potential to change the stream power of a river and in catastrophic cases create a landslide-dam, changing in fact the morphology of the valley [Korup, 2005], [Korup and Schlunegger, 2007].

The geomorphological analysis and mapping of the Calanca valley by Seiffert [Seiffert, 1960] is still the only general publication about the region.

1.2 Study area overview

The Calanca valley, located in southern Graubünden, Switzerland, is a confined alpine valley prone to landslides and rockfalls of various size (e.g. single blocks through to debris avalanches up to 30000 m^3) and offers the opportunity to study the influence of landslides and rock falls on stream bed development and valley morphology. This study will focus on the southern section of the Calanca valley, between Buseno and Cauco (see Figure 1.1). The river of the Calanca valley is called *Calancasca*.

According to the Tectonic and Petrographic Map of the Central Lepontine Alps [Berger et al., 2007], the study area is located within the Adula nappe (Paleogene tectonic accretion channel) and the Simano nappe (European basement). Both the nappes belong to the Penninic domain.

1.3 Research objectives

The objective of this project was to understand if there was a correlation between landslides within the studied region, the river profile and the river's dynamics. The study focused particularly on the following points:

1. Analyse the long river profile in relation to the occurrence of landslides and rock falls in the Calanca valley and determinate how they have modified the river inclination.

2. Analyse the river dynamics and determinate the return period of extreme events that have sufficient energy to transport rock debris originating from landslide and rock fall activity.
3. Evaluate whether a debris avalanche was involved in creating a landslide-dam at the valley narrowing around Selma in the Calanca Valley.

This complex problem involves at least three simpler subsystems (landslide, river-profile and river-dynamics) that could influence each other. We choosed to split it and to analyse individually each subsystem. It is important to notice that the most delicate subsystem is the river-profile, because it links the geology, i.e. the landslides, with the hydrology, i.e. the dynamics of the river. Important relationships are highlighted in Figure 1.2.



Figure 1.1: Studied area, modified after [Fossati, 2008]

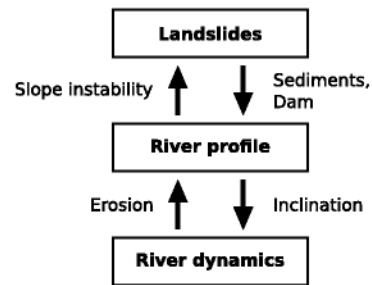


Figure 1.2: Possible relations between the subsystems

Chapter 2

Data

2.1 Digital models

The long river profile is the connection element between the geology and the hydrology, therefore it is important to measure it accurately. There are various possibilities to do this, for example - in order of decreasing accuracy - a Differential Global Positioning System (DGPS) measurement, a theodolite-measurement, and then the Federal Office of Topography (*Swisstopo*¹) Digital Terrain Models (*DTMs*).

Swisstopo provides two *DTMs*. The first one is named *DTM-25*, has an horizontal resolution of 25 *m* and in the studied area a vertical accuracy of 1 *m*. The second one is a new technology, it is called *DTM-AV*, has been made with laser-scans (LIDAR) from airplanes and reaches an horizontal resolution of 2 *m* with an accuracy of 0.5 *m*. In order to avoid the presence of clouds and snow these type of scans are generally made during the summer period. Unfortunately this could have the disadvantage that at the end of the summer some alpine lakes contain less water and could therefore look like depressions containing a sinkhole, which in a gneiss-predominated region would not make sense.

During the laser scanning the signal is reflected more than once, because of the barriers with different coverage that he can hit during his path, e.g. soil, water, trees. In a digital terrain model this return signal is usually filtered in order to get a better approximation of the real terrain model. The filtering process includes the removal of vegetation (the first return signal is removed), buildings (using updated maps from the land registry office and orthoimages), etc. However, this process is not perfect and some errors remain. It is also important to note that the laser is not able to penetrate through a water column.

2.2 Streamflow

The Federal Office of Environment *BAFU* ² also takes care of the monitoring of rivers, lakes and groundwater bodies, providing long-term hydrological data of water levels, discharge, bed-load, suspended sediment, temperature, oxygen, conductivity, etc. It also owns a measurement-station located before the village of Buseno, the lower part of the catchment. This collected Calancasca's daily streamflows since 1952 and hourly streamflows since 1974.

¹<http://www.swisstopo.admin.ch/>

²<http://www.bafu.admin.ch/>

2.3 Field observation

Field work was undertaken from 6th to 7th May and from 11th to 12th June 2009 and included mapping and measurements. This included particularly the measurement of various river's cross sections, the measurement of the grain-size in two places dominated by clasts of gravel respectively of the boulder-size, the mapping of the river's erosion dynamics, the mapping of the sedimentology of the bed river and the mapping of the morphology of a smaller region of the studied area, where many blocks lie over the river bed. The field work allowed us also to better understand the dynamics of the system.

2.4 Cartographic material

We also used standard cartographic material, i.e. the 1:25'000 Swisstopo topographic maps and the Swisstopo orthoimages (Swissimage), with an horizontal resolution of 0.5 m . All the topographic maps and the orthoimages were digitalized and georeferenced.

Chapter 3

Methods

3.1 River profiles

3.1.1 Long river profile

The long river profile is normally a plot of the elevation z of the points along the whole river length l . This study was limited to a river-portion of only approximately 8 km length, therefore with the term *long river profile* we will hence refer only to the studied part of the whole river profile. The long river profile plays a central role in this study because it links the geology to the hydrology: a rock-failure event could act as natural dam, building a lake, which sedimentation could lower the upstream gradient of the long river profile. Such a decrease in the steepness in the zone of the lake and the following suddenly increase of the slope, which is due to the dam, can act as crucial factors for the hydrological-regime.

For the extraction of the long river profile we used the *Create Profile Graph* utility of the *ArcGIS*'s (a commercial Geographic Information Systems program that allows to manipulate both raster and vector graphics, e.g. topographic maps, orthoimages, digital models, etc.) *3D-Analyst toolbox*. This function interpolates the line of the river with the height of a digital model, creating a plot of the length l vs the elevation z . The data of this profile can be exported in a *.csv* file, a matrix of all the values of l starting from 0 with their corresponding values of z . This permits to later import the data in *Matlab* (a numerical computing program) to easier manipulate and plot it. The river's drawing process is a delicate and crucial phase, because of the high accuracy of the DTMs.

Manual drawing A first possibility is to manually draw the river's path over a digital model, trying to follow the steepest path of the DTM, that usually has a better accuracy than orthoimages and topographic maps, but also to move around the various obstacles (banks, blocks, ..) that lie in the river bed. This method could sound rough, but has the advantage to force a user to look at the inaccuracies of the models that are never perfect. It allows also a user to find a compromise between following the model and the reality (orthoimages, field observations, etc.).

Hydrological calculation ArcGIS provides a powerful tool to automatically draw the path of a river. This method is based on simple hydrological calculation and can be resumed with the following steps (in slab-serif the name of the ArcGIS functions).

- Fill all the holes of the digital model, letting each cell drain downstream without any doline-cell.
`Fill_sa`
- Calculate the flow direction (the steepest one) of each cell.
`FlowDirection_sa`
- For each cell calculate the number of cells n that drain on it.
`FlowAccumulation_sa`
- Define the river-path as the sequence of the cells where $n > \text{value}$. *value* is a constant that depends of the model.
`con(flow_acculation > value)`

With both these methods a plot of the data shows a lot noise (see Figure 4.3). Especially as we derived the profile to obtain the valley's slope the noise was dramatically amplified and the real slope became not identifiable, therefore we considered two possibilities to avoid this. A first possibility is to find a function that fits the data, a second one to smooth the signal.

Data fitting As Fourier showed in 1807 every periodic function can be decomposed in an infinite sum of sines and cosines, called Fourier transformed. This processes over a discrete signal that is called discrete Fourier transform (DFT). As the long river profile is a complex curve the only low grade function able to approximate it could be a discrete Fourier transformed. Matlab provides a powerful function called `fit` that fits data with a discrete Fourier transformed, but unfortunately this DFT is limited to the 8th degree, which is insufficient for the number of knickpoints present in the signal. Also the standard DFT function (called `fft`, Fast Fourier Transform) was not able to fit the data, because the calculated function showed big oscillations at the begin and at the end of the signal. This is a known disadvantage of the DFT process and is due to the convolution with the rectangular window function. Indeed the function calculated with Matlab's `fit` function did not show these oscillations, which means that it must include an extra filter to avoid this.

Data smoothing In signal processing a low-pass filter is a filter that reduces the amplitude of the high frequencies of the signal's spectrum but that lets pass the low frequencies. There are many algorithms to undertake this analyse and I used a combination of the following three:

- Pit filling is a procedure commonly used in hydrology. It consists in avoiding cells surrounded by cells with higher values. This is basically an error correction process. Such an algorithm for a 2D object like a long river profile is quite simple. This is an example of code for Matlab that fills the pits of a decreasing long river profile, where l is the length and z the elevation.

```
for i=2:length(l)
    if( z(i) > z(i-1) )
        z(i) = z(i-1);
    end
end
```

- A common method used for the reduction of signal's noise is the *median filter*. Let k be the k -st point of the signal and s the filter's window size, then the filtered value of k will be the median of all the points of the interval $[k - s + 1; k]$. For this task I used the `medfilt1` of Matlab.
- Another method is the *simple moving average (SMA)*. It consists in the un-weighted mean of the previous n data points. Let k be the k -st point of the signal and s the filter's window size, then the filtered value of k will be the un-weighted mean of all the points of the interval $[k - s + 1; k]$. This can be expressed with the following equation:

$$SMA_i = \frac{x_i + x_{i-1} + \dots + x_{i-s+1}}{s}$$

Also this function is implemented in Matlab and is called `filter`.

The median filter is a powerful tool for noise reduction but if it is used with big window sizes, it tends to destroy also the real variations in the long river profile signal, especially the biggest peaks of the derivative. Indeed the SMA was less efficient in the noise removal, but it was possible to apply it also with big window sizes without destroying the signal. After some tests with the data exported from the DTM-AV we finally decided to apply at first the pit-filling filter, then a median filter with a window size of 10 points and at last an SMA filter with a size of 100. With the data from the DTM-25 I did the same, but with an SMA with a window of only 20 values, because of the lower resolution of this model. For all the derivative I added an extra median filter of 10.

This combination of filters is a good compromise because it eliminates most of the noise without losing the real information of the long river profile. Filter it with bigger window sizes erases more noise but damages also the signal, e.g. the biggest values of the slope decrease from 8° to $4 - 6^\circ$.

3.1.2 Cross sections

A cross section is a profile cross to a river. Cross sections are the results of complex geomorphologic interactions and influence both the hydrology and the geology but can also be influenced from them. For example cross section's area and wetted perimeter influence the backwater curve (the height of the water columns over a long river profile, see Chapter *Backwater-curves algorithm*) but a steep cross section could cause a rock failure. As this study focuses more in the ability of the river to transport the material, we measured only the geometric parameters of the cross sections necessary for the calculation of the area and the wetted perimeter, i.e. b_1 , b_2 , b_3 , a_1 and a_2 (see Figure 3.1). Measurements have been made with a *Leica locator*, a special laser binocular able to measure distances and angles within objects. It could measure distance from 1 m to 2000 m with a precision of approximately 0.5 m. Measurements have been made in 17 points between Cauco and Arvigo choosed with various criteria, i.e. changes in the geometry, in the morphology, in the sedimentology or in the slope (see Figure A.6).

3.2 Geological analysis

3.2.1 Sedimentology of the river bed

A simple but powerful river-classification consists in separating transport-limited from detachment-limited channels [Tucker and Whipple, 2002]: in transport-limited channels

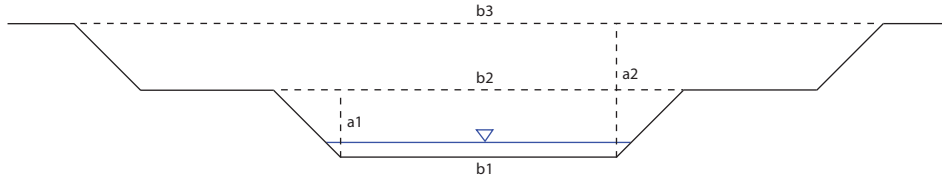


Figure 3.1: Parameters measured in the cross sections

the erosion is limited by the local transport capacity and in detachment-limited the incision only depends on the bed shear stress which is function of the elevation of the water column. This classification can be made looking at the material deposited in the river: during periods of low streamflow transport-limited channels are characterized by the presence of sediments, e.g. gravels, cobbles or boulders that lie on the bed river. However, detachment-limited channels are almost not covered by sediments so that the bedrock can outcrop. This classification permits to understand the general regime of the river.

In order to get an idea about the river's energy, a sediment-map was also necessary. There is no 1:25'000 geological map that covers the Calanca valley and the only available 1:50'000 map (Geologische Karte der Adula, 1920) covers just the northern part of the valley and does not reach the studied area. Therefore the only available map is the 1:100'000 Tectonic and Petrographic Map of the Central Peponine Alps [Berger et al., 2007]. For this reason we had to determine the sedimentology of the river ourselves: field investigations included also the mapping of the different sedimentation zones along the long river profile. As this study focuses more on the erosional potential, we were mainly interested in the mechanical behaviour of the different sediments, therefore we opted for a classification based on dominant grain-size. To estimate the grain-size we looked at the b-axis of a clast, which means at its middle-long axis. The description of the clast is based on the nomenclature guidelines of [Matula, 1981] and the grain-size classification on [Blair and McPherson, 1999].

The results of river's regime balance are summarized in the map of Figure A.1, and the results of the sediment-classification in the maps of Figures A.2, A.3 and A.4.

We were also interested in investigating the presence of sediments associated with the formation of a lake in the interior parts of the alluvial plane of *Pian di Gamb*, in the north of Selma. Therefore we contacted many people of the Office for Nature and Environnement of Chur asking for the stratigraphic sequence of the piezometer built for research purposes in *Pian di Gamb*, but nobody knew if one had been made. Unfortunately this investigation could not be concluded because of time constraints.

3.2.2 Morphology

In order to understand the genesis of the big clasts that lie on the river bed, I needed a detailed geomorphological map of the valley sides between Arvigo and Selma. The only geomorphological study in this region is the geomorphological map of the Calanca valley carried out by [Seiffert, 1960]. However, due to the large area covered by the map (scale 1:25'000), Seiffert had to simplify the geomorphological structures, therefore the map lacked details for this study and we decided to map one ourselves.

The 2m-resolution of the DTM-AV permits to observe variations in the elevation caused by the presence of clasts up to a size of 3-4 m (which corresponds to very coarse boulders and blocks, see Table 4.1). The location of the area with blocks and boulders

on the morphological map was also derived from the digital model.

3.3 Hydrological analysis

Hydrological analysis are necessary to understand the river's behaviour, and particularly to calculate the occurrence-probability of the streamflows of high magnitude. Such streamflows, also called *extreme events*, can mobilize large quantities of sediments, and in places where cross section's areas become too small can also flood over the sides, causing important changes in the geomorphology. As the daily data covered a larger period (57 years) than the hourly ones (31 years) we decided to analyse them.

3.3.1 Periodicity

Understand the periodicity of a data set is a central point, because it permits to understand the process but also to better isolate the periodical extreme events. The periodicity of the streamflow seemed to be of one year, a typical value for a river's streamflow period. To be sure about it and to check if the signal also had some other smaller and therefore invisible periods, we analysed the amplitudes of the Fourier spectrum. To do this we used the Matlab's algorithm for the discrete Fourier transform (`fft`), which returns a vector with the coefficients of the discrete Fourier transformed. The periodicity can be determined analysing the peaks of a plot with increasing frequencies (from 0 to the Nyquist frequency FN) versus the absolute values of their coefficient's amplitudes. If the signal is periodic over the whole data set with frequency f , the plot of the magnitude of its Fourier transformed contains a peak by f .

```
N = length(x);
FS = 1;                                % sampling frequency [1/d]
FN = FS/2;                             % Nyquist frequency [1/d]
Nf = N/2 + 1;                          % # plotted coefficients

X = fft(x);
f = linspace(0,FN,Nf);

plot(f,abs(X(1:Nf)));
```

3.3.2 Probability

The *probability density function* (PDF) and the *cumulative density function* (CDF) have been calculated for the daily streamflow signal. The yearly *exceedance probability*, which for extreme events corresponds to the *flood probability*, has also been calculated for it.

Empirical daily PDF The empirical daily PDF can be calculated by counting the events within intervals of $1\text{ m}^3\text{s}^{-1}$ and dividing them with the total amount of data.

Empirical daily CDF The empirical daily CDF can be calculated in a similar way, but the probabilities are summed together in order to obtain the cumulative probability.

Yearly exceedance probability The binomial distribution can be used to convert daily to yearly probabilities. The probability that an event X of probability p occurs k times over n independent tests can be calculated with the Binomial law:

$$P(X = x) = \binom{n}{x} \cdot p^x \cdot (1 - p)^{n-x} \quad (3.1)$$

Let now X be the random variable for a daily streamflow of magnitude x , then its daily CDF is defined as $p_x = P(X < x)$. Let now Y_x be the random variable of the yearly exceedance of the same event x . The yearly exceedance probability is defined as the probability that over one year an event occurs at least once ($P(Y_x \geq 1)$), and using Equation 3.1 for $Y_x = 0$ can be simplified as follows:

$$p_{Y_x} = P(Y_x \geq 1) = 1 - P(Y_x = 0) = 1 - P(X < x)^{365} = 1 - p_x^{365}$$

This means that the yearly exceedance probability (p_{Y_x}) of an event of magnitude x can be calculated directly from the daily CDF (p_x).

3.3.3 Extreme event analysis

An extreme event analysis is used to determine at which frequency an extreme event (EE) can happen. To do this it is necessary first to isolate the EE and then to calculate its exceedance probability.

Isolation of the extreme events EEs can be isolated using the *annual peaks* method, which consists in taking for every year the biggest peaks as one EE. It is well known that a system such a river can have more than one probability distribution for events of different magnitude, i.e. one for usual streamflows and a second one for EEs. The peaks have been isolated from the daily streamflows with the annual peaks methods, therefore the EE-dataset consisted in only 57 EEs, one for each year of the period 1952-2008. However, 57 values are too less to calculate an empirical exceedance probability, therefore we searched for a probability distribution that was able to fit the EE.

Plotting position This is a technique to graphically test if a postulated distribution fits the data. Let $G(x)$ be the proposed CDF for the observations X and U_i the exceedance probability of the i th element. According to [Maidment, 1993] the value of $X_i = G^{-1}(1 - U_i)$ should be nearly $G^{-1}(1 - q_i)$, where q_i is our estimation for U_i . This means that in a plot with $G^{-1}(1 - q_i)$ vs X_i the points would lie on a straight line only if $G(X)$ fits the data.

Weibull plotting position A classical method called *Weibull plotting position* requires an estimation of the exceedance probability by sorting in decreasing order the EEs:

$$x(n) \geq x(n-1) \geq \dots \geq x(1)$$

To the i th largest event the exceedance probability is estimated as follows:

$$q(i) = \frac{i}{n+1}$$

Gumbel distribution The *Gumbel distribution*, also called *EV type I*, is one of the extreme value (EV) distributions described by [Gumbel, 1958]. As documented in [Maidment, 1993] for the Gumbel distribution $G^{-1}(1 - q_i) = \xi - \alpha \cdot \ln(-\ln(1 - q_i))$. This lets us simplify considerably the plotting procedure, i.e. plotting the *reduced Gumbel variable* y_i vs x_i .

$$y_i = -\ln(-\ln(1 - q_i))$$

Return period Once the EE-distribution is known, it is necessary to calculate parameters that usually depend on the mean and the variance of the data x . According to [Maidment, 1993], the CDF of the Gumbel distribution is defined as:

$$P(X \leq x) = F(x) = e^{-e^{-\frac{x-\xi}{\alpha}}} \quad (3.2)$$

where the parameters ξ and α can be calculated solving the following system of equations containing only coefficients and variance and mean of the values:

$$\begin{aligned} \mu_X &= \xi + 0.5772 \alpha \\ \sigma_X^2 &= 1.645 \alpha^2 \end{aligned}$$

Now it is finally possible to calculate the exceedance probability for any EE using the theoretical formula of the CDF, e.g. for the Gumbel distribution using (3.2). The yearly exceedance probability U_i of an event x_i is identical to $1 - F(X = x_i)$ and the return period (in years) can be defined as

$$T_i = \frac{1}{U_i} = \frac{1}{1 - F(x_i)}$$

3.4 Hydrological modeling

To link together the hydrological data and the geological observations I needed to estimate the shear stress τ along the long river profile. As the shear stress is function of the water depth h I needed a hydrological model to calculate the *backwater curve*, which means a plot of the height of the water column along a river profile.

I decided to simplify the situation assuming steady and subcritical flow conditions. *Steady flow* means that the flow and the velocity is constant over the time. *Subcritical flow* signifies that the inertial forces dominate over the gravitational ones. Mathematically this happens when the *Froude number* Fr is lower than 1, otherwise the flow is called supercritical.

$$Fr = \frac{v}{\sqrt{g h}}$$

In the case of a subcritical flow, the stream is slow enough to propagate flow disturbances upstream, therefore the simulation of the backwater curve must start at the end of the river.

3.4.1 Backwater-curve's algorithm

In order to better understand the simulation-mechanism, I decided to write my own code. The most known program to calculate backwater-curves is *HEC-RAS* (River Analysis System), which has been developed by the Hydrologic Engineering Center (HEC) of the United States Army Corps of Engineers, therefore I decided to base my program on their documentation [Various, 2008].

The algorithm is based on the energy balance equation:

$$z_2 + h_2 + \frac{v_2^2}{2g} = z_1 + h_1 + \frac{v_1^2}{2g} + h_{L,1} \quad (3.3)$$

Where z_i is the river bed elevation, h_i the height of the water column, v_i the stream-velocity and $h_{L,i}$ the energy loss for the point i ; g is the gravitational acceleration.

Normally the *energy loss* h_L between two cross sections should include both the friction loss and the contraction or expansion loss, but for this study we decided to consider only the friction loss. The energy loss equation is:

$$h_L = L \bar{S}_f \quad (3.4)$$

where L is the horizontal distance between two cross sections and \bar{S}_f the average friction slope between them.

There are many ways to calculate \bar{S}_f , one of the most common is to use the *average conveyance equation*:

$$\bar{S}_f = \left(\frac{2Q}{K_1 + K_2} \right)^2 \quad (3.5)$$

Q is the streamflow which is assumed to be constant over the whole river and K_i is the *channel conveyance factor* which can be calculated with the *Manning's equation*:

$$K_i = \frac{1}{n} A_i \left(\frac{A_i}{p_i} \right)^{2/3} \quad (3.6)$$

n is the *Manning's roughness coefficient* and depends on the material that lies in the river bed but also on the river's geometry. A_i is the cross section's area and p_i the wetted perimeter of the cross section.

The last equation used by the algorithm is the flux definition:

$$Q = v A \quad (3.7)$$

Let now i be a point where only the river bed elevation z_i is known and $i - 1$ a point downstream where v_{i-1} , z_{i-1} and h_{i-1} are known. It is possible to calculate the water depth in i using the following procedure:

- Estimate a water depth $h_{estimated,i}$ for the point i .
- Calculate the river's area A_i and the wetted perimeter p using the estimated value of $h_{estimated,i}$.
- Calculate the velocity v_2 using (3.7) with the constant-assumed streamflow Q .
- Calculate the channel conveyance factor K_i using (3.6).
- Calculate the average friction slope \bar{S}_f using (3.5).
- Calculate the energy loss h_L using (3.4).
- Calculate the water depth $h_{calculated,i}$ that would result from the energy balance at the previous calculated condition using (3.3).

- Calculate err , which is the difference between the calculated water column $h_{calculated,i}$ and the estimated water column $h_{estimated,i}$.

With the previously calculated error it is now possible to make a better estimation, e.g. $h_{estimated,i} + 0.7 err$, and then to cycle the procedure until the error becomes lower than a tolerance-value.

Thanks to this method, choosing some boundary conditions such a constant stream-flow Q and the river's height at the start-point h_0 , it is possible to reconstruct the back-water curve by cycling through all the points i of the whole long river profile calculating the water elevations h_i .

This algorithm have been implemented in Matlab and the source code is available at Appendix B.1. This program load a file containing a matrix, which lines have the following space-separated structure: "l z b1 b2 h1 b3 h2 N o". l is the horizontal distance, z the elevation, b_1, b_2, h_1, b_3, h_2 the previous described cross-section's parameters and N the Manning's roughness coefficient. All the previously mentioned values are float numbers and are essential for the calculations. o is an optional boolean value and in the places where it is set to 1 the program draws a vertical line. This could be useful to evidence important points in the plots, e.g. the points where the sections change. Before to run the program it is important to set realistic boundary conditions in the `main.m` file, i.e. the constant flow Q and the water elevation at the start point $h(1,1)$, as well as the name of the file that contains the data.

3.4.2 Sediment motion

The critical conditions for the initiation of sediment motion is called *incipient motion*. This happens when the forces that act on the grains exceed the resistance forces. According to [Shields, 1936], when the only forces are the fluid force and the resistance of the cohesionless particles, the incipient motion starts when

$$\tau_* = \frac{\tau_0}{(\rho_s - \rho_f) g d_s} \approx 0.5$$

Where τ_* is the ratio between inertial and gravitational forces, τ_0 the *fluid shear stress*, ρ_s and ρ_f are the densities of the sediment respectively of the fluid, g is the gravitational acceleration and d_s the grain-size. For a quartz-rich sediment $\rho_s \approx 2700 \text{ kg m}^{-3}$ and for a river-water density $\rho_f \approx 1000 \text{ kg m}^{-3}$, therefore the previous equation can be simplified as follows:

$$\tau_0 = 0.5 (2700 - 1000) \left[\frac{\text{kg}}{\text{m}^3} \right] 9.81 \left[\frac{\text{m}}{\text{s}^2} \right] d_s [\text{m}] \approx 8340 d_s \left[\frac{\text{N}}{\text{m}^2} \right] \quad (3.8)$$

The fluid shear stress of a river is defined as the stress that the water column applies tangential to the river path and for low angles can be approximated as follows [Maidment, 1993]:

$$\tau_0 = \rho_f g h S \quad (3.9)$$

S is the river slope, therefore the minimal shear stress needed to start moving sediments of a certain size only depends on the water column h and on the derivative of the long river profile $S = dz/dl$.

Chapter 4

Results

4.1 Geological results

4.1.1 Sedimentology of the river bed

After the first walk down along the river we already realized that there were zones of totally different transport regimes, e.g. transport- and detachment-limited channels, and that also within this zones - specially in the transport-limited channels - the grain-size was quite variable.

Transport- vs detachment-limited channels This first mapping process was quite trivial, because - except of the artificial channels - in the studied area there is only one long detachment-limited channel of 2010 *m* that begins in Selma (P_1 on the map) and ends 1850 *m* before the Buseno lake (P_2 on the map). It is characterized by bedrock, with only a thin layer of sediments covering the almost constant outcropping rocks, i.e. gneiss. The rest of the studied area is covered with a variety of sediments and must therefore be transport-limited. Only short after Arvigo the otherwise almost homogeneous detachment-limited channel is interrupted by a small zone where the river bed is covered by boulders, but this is due to the rock-waste that comes from the close gneiss surface-mine. These results have been summarized in the map of Figure A.1.

Sediment map The second subdivision was based on grain-size distributions. In general the sediments are typical unconsolidated fluvial sediments. Deposits are poorly sorted: in many places it is possible to find sand, gravel and cobble and often also fine and medium boulders (for the grain-size nomenclature we will refer to Table 4.1). Because of this heterogeneity we decided to subdivide the sediments in only two large categories: *cobble-dominated* (about 60 % Vol cobbles) and *boulder-dominated* (about 50 % Vol boulders), see maps of Figures A.2, A.3 and A.4.

- The cobble-dominated sediments (in green in the maps) are the most common and appear in the three maps. Clasts are rounded, flat, smooth and poorly sorted: even though they are cobble-dominated, they also contain smaller (about 30 % Vol, from gravel to sand, see Figure 4.1 - A) and coarser (about 10 % Vol, up to coarse boulder) components. In these zones the river usually develops a higher sinuosity and tends to build banks (see Figure 4.1 - B). These sediments are mostly located in the river bed while the valley sides are often covered by soil and old woods.

- The block-dominated sediments (in blue in the maps) are concentrated in only two small regions north of Arvigo (see Figure 4.2 - A). In contrast to the cobble-dominated sediments this lithology covers also the sides of the valley up to some rock walls. Moreover, these sediments are subangular, irregular, smooth and not sorted. In other words, the smaller clasts and the submerged part of the blocks that lie on the river bed are subrounded (see Figure 4.2 - A), while all the others located over the sides are subangular (see Figure 4.2 - B). Like the others also these sediments are poorly sorted: commonly on the sides of the river bed it is possible to observe small banks of sand and granules within bigger heaps of pebbles (together about 10 % Vol). Bigger clasts (cobbles and boulders) cover both the river bed and the valley sides and build about 40 % Vol. However, the volume of this sedimentation-zone is clearly dominated by the huge amount of blocks, the biggest of which have a volume of approximately 1000 m^3 (see Figure 4.2 - C).
- The previous mentioned bedrock has also be mapped (in red on the maps). In this region the bedrock is an amphibolite gneiss. In the whole valley the gneiss-foliations are steep and east-oriented, this can explain the higher concentration of rock-failures on the right side of the valley [Seiffert, 1960]. Bedrock is present only in the map of Figure 4.1 - C.
- The last mapped unit are the artificial channels (in pink). In the past these stretches have been modified by humans, therefore they could indicate potential regions of instability in the erosion/sedimentation balance that forced the local people to solidify the embankments.

Fraction	Class	Grade	Size	Map-colour
sand			1-2 mm	
gravel	granule pebble		2-4 mm 4-64 mm	
	cobble		6.4 - 25.6 cm	green
	boulder	fine medium coarse very coarse	25.6 - 51.2 cm 51.2-102.4 cm 102.4 - 204.8 cm 204.8 - 409.6 cm	
megagravel	block slab		4.1 - 65 m 65.5 - 1049 m	blue

Table 4.1: grain-size, modified after Blair [Blair and McPherson, 1999]



A)

Cobbles and gravel
(Pian di Gamb)



B)

Cobbles
(Pian di Gamb)



C)

Bedrock
(downstream from
Arvigo)

Figure 4.1: Field photographs



A)

Block-dominated
sedimentats
(Isolan)



B)

Block on a valley side
(Isolan)



C)

The largest block
(Isolan)

Figure 4.2: Field photographs

4.1.2 Long river profile

Comparison of profile techniques Figure 4.3 is the plot of the original signals exported with ArcGIS. There are three signals plotted because they have been extracted from different river paths. Two of these lines have been calculated with the previous described hydrological algorithms, one using the DTM-AV model (in blue in the plot), the other one with the DTM-25 (in red). The third path has been manually drawn and has been interpolated over the DTM-AV (in green). In ArcGIS both the calculated (but not the drawn) river's paths started and ended at the same points, but in the plot it is evident that the blue line is about 1 km longer than the red one. This is due to the best resolution of the DTM-AV that allows the hydrological calculated river's path to develop meanders that result in a longer path, as visible in the map on the right of Figure 4.4. Another observation about this map is that at its top also the manual drawn path follows a big meander like the calculated DTM-25. However, in the map on the left of the same figure the calculated DTM-AV path leaves the real river crossing the Pian di Gamb plain, while the manual drawn line follows the river over a smooth profile. These are examples of how the manual-drawing process can be a very good compromise between the digital model (in this case the DTM-AV) and the reality (the orthoimages and eventually the topographic maps).

Returning to the long river profile, a second important observation is that the signal of the inclination, which is a way to express the changes over the profile, includes a lot of noise that significantly increases from the DTM-25 to the two DTM-AV data. Both the DTM-AV contains noise of a similar magnitude, but the self-drawn has some really big peaks. Anyway such extreme variations can be very well filtered by a median filter.

Description Figures 4.5 and 4.6 represent two analyses of the long river profile. In the first figure the data comes from the manual drawn and over the DTM-AV interpolated path. This figure also contains the sequence of the sedimentology along the river profile. The data of the second figure comes from the hydrological calculations with the DTM-AV. In both the figures there are two plots, the first of them is a standard long river profile, with the length l vs the height h . The second represents the inclination (in degrees) $\alpha = \arctan(\Delta h / \Delta l)$ of the river along the length l .

The following description of the long river profile is valid for both Figures 4.5 and 4.6. The long river profile shows a stepwise decrease with small waterfalls and pools. Points where the inclination rapidly changes are called *knickpoints* and in the plot are labeled with the letter k , while the points of minimum-slope are labeled with the letter m . Point k_1 represents the end of *Pian di Alne*, a large plain before Cauco, and the begin of a very steep zone that reaches a slope of 5.8° (for slope-values we well refer to the values of Figure 4.5). This ends in *Pian di Gamb*, the plane before Selma, where the slope decreases to about 0.6° . The knickpoint k_2 represents the end of this plane: the slope increases gradually until a zone with a slope of about 2° . This zone is perturbed by two big anomalies, i.e. the knickpoints k_3 and k_4 , where the gradient suddenly jumps to very high values (4.4° resp. 3.9°). These two points correspond very well to the begin of the two areas of block-dominated sediments. The river reaches then a second flat zone, the plain of Tandet, where m_5 is its point with the lowest slope. After this plain the river's inclination suddenly increases by the knickpoint k_6 , which lies at the height of the bridge of Arvigo, reaching 5.2° , one of the highest slopes. This point also correspond to the begin of the erosional zone and to the only real lithological boundary of the study area: granitic gneiss (to the north) borders on polycyclic gneisses with amphibolite (to the south) [Berger et al., 2007]. Downward also in this bedrock-

zone the slope decreases until another low value (m_7), the only point of the erosional area where the channel has been artificially fortified. Later the river's slope increases and it begins a sedimentation zone, but then the inclination decreases again until the slope-minimum of m_8 . It is interesting to notice that at this point there is another small erosional zone within an almost constant sedimentation area.

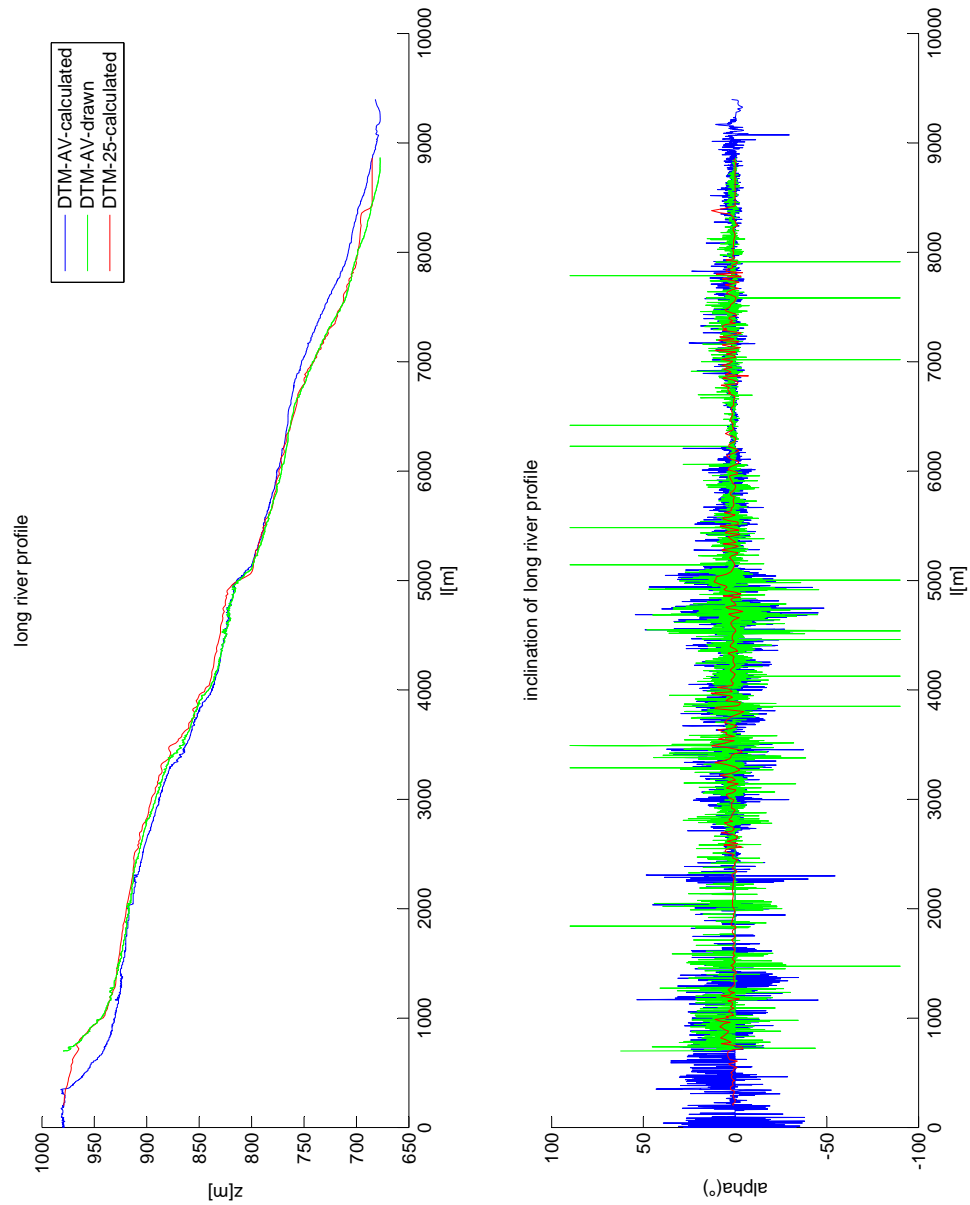


Figure 4.3: Comparison between non-filtered profiles extracted by different models and with different techniques

4.1.3 Morphology

The main morphological structures that I found in the studied area have been *alluvial planes*, *rock-avalanches* and *rock-failures*.

There are two alluvial planes in the studied area: the previous mentioned *Pian di Gamb* is located northern of Selma and *Tandet* northern of Arvigo. The sediment of these alluvial planes (at least in the bed river) does not differ much from all the other cobble-dominated areas, therefore I classified them together. *Pian di Gamb* (about $1000 \times 300 m^2$) is larger than *Tandet* (approximately $500 \times 150 m^2$). *Pian di Gamb* also appears more developed than *Tandet*: it expands itself at both sides of the river and is crossed by various brooks that lie parallel to the main river. These brooks could be a natural drainage developed by the flood plain but are more probably artificial channels constructed by humans to quicker drain their cultivated fields. However, *Tandet* covers mostly the left side of the valley and is crossed only by some small tributary brooks.

There are three sites, very close to each other, where rockslides cover the side of the valley and reach the river bed. These rockslides are mainly composed of fragments within the block of the coarse-boulder grain size. The first two zones (*Isolan* on the left and *Gagna della Scranna*) are on opposite side of the river channel and correspond to the first block-dominated sediment-unit and to the knickpoint k_3 . The third rockslide (*Miaddi*) extends itself only on the left side of the lowest block-dominated unit and corresponds to the knickpoint k_4 . The three rockslides are mainly covered with mature forest made of conifers, but the vegetation progressively decreases toward the highest sides of the valley, which could indicate an ongoing rock-fall activity. The morphology of this area is summarized in the map of Figure A.5.

4.1.4 Cross sections

The previous described cross section parameters have been measured in 17 localities between Cauco and Arvigo (see the map of Figure A.6). All the measured data are available in table A.1, but for the simulation we decided to simplify the situation.

We found that there are mainly three type of channels: A, B and C, with the followings features:

- A. **Wide and deep.** These are very wide (in some places b_3 reaches $100 m$) and deep ($a_2 = 10 m$) channels. There is only one stretch with this characteristic (a).
- B. **Wide and flat.** This cross section shape is typical of alluvial planes. In the studied area there are two of these channels: one by *Pian di Gamb*, the second one by *Tandet*.
- C. **Narrow** In these stretches many blocks obstruct the main channel, therefore the river develops small meanders and flows around them. These new channels are narrow ($b_1 < 5 m$) but quite deep ($6 m < a_2 < 7 m$). There are two of these channels and they correspond very well to the block-dominated channels.
- D. This channel is a transition zone between type-B and a type-C zones. In these stretches the channel progressively becomes narrower and deeper.

According to this classification and using the measured cross sections the river between Cauco and Arvigo has been divided in seven stretches (a, b, c, d, e, f, g). For each stretch the cross section's parameters have been calculated as the mean of its measured parameters. Table 4.2 resumes the classification of the sections and the approximations of the parameters.

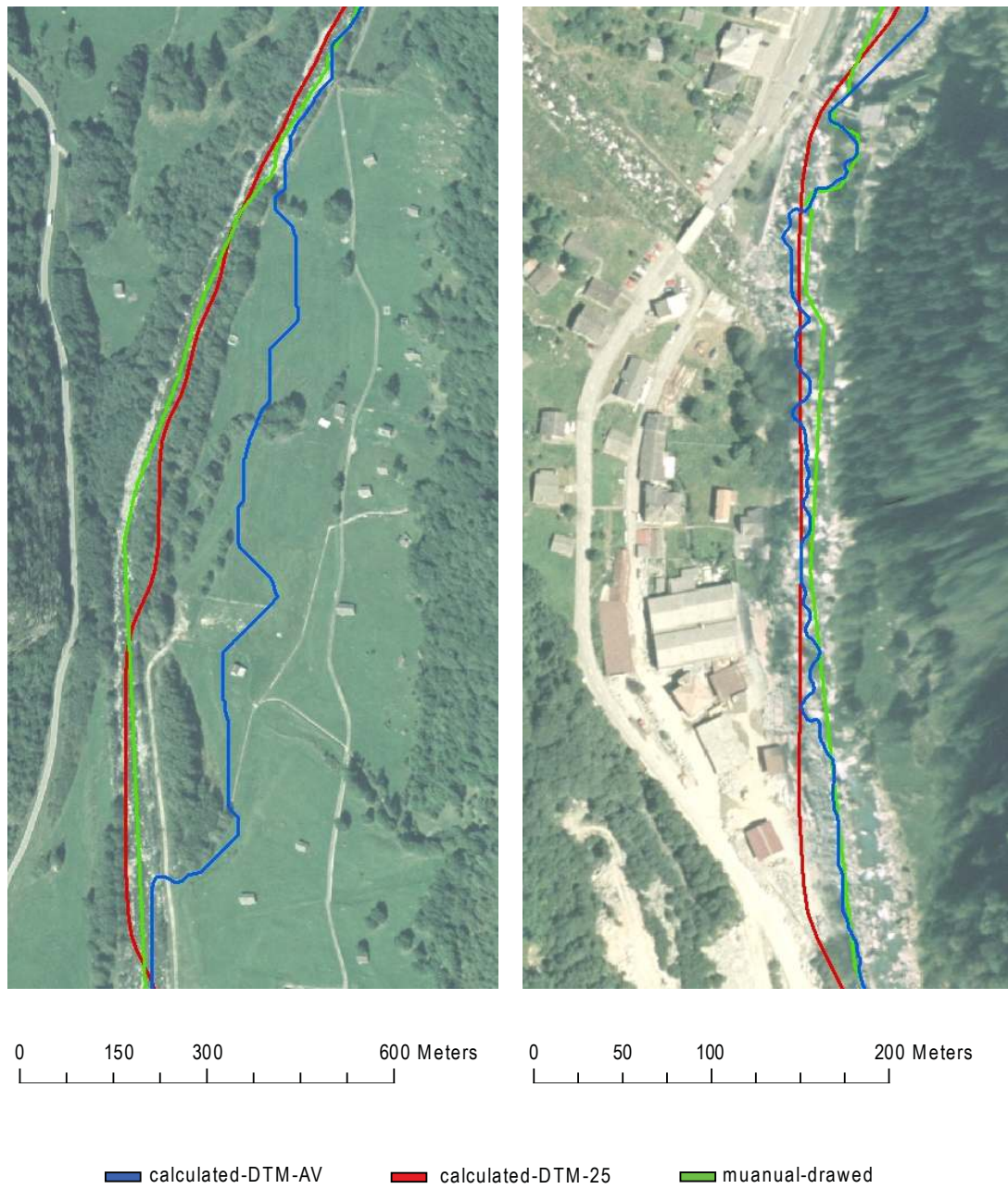


Figure 4.4: Comparison between river paths drawn with different methods

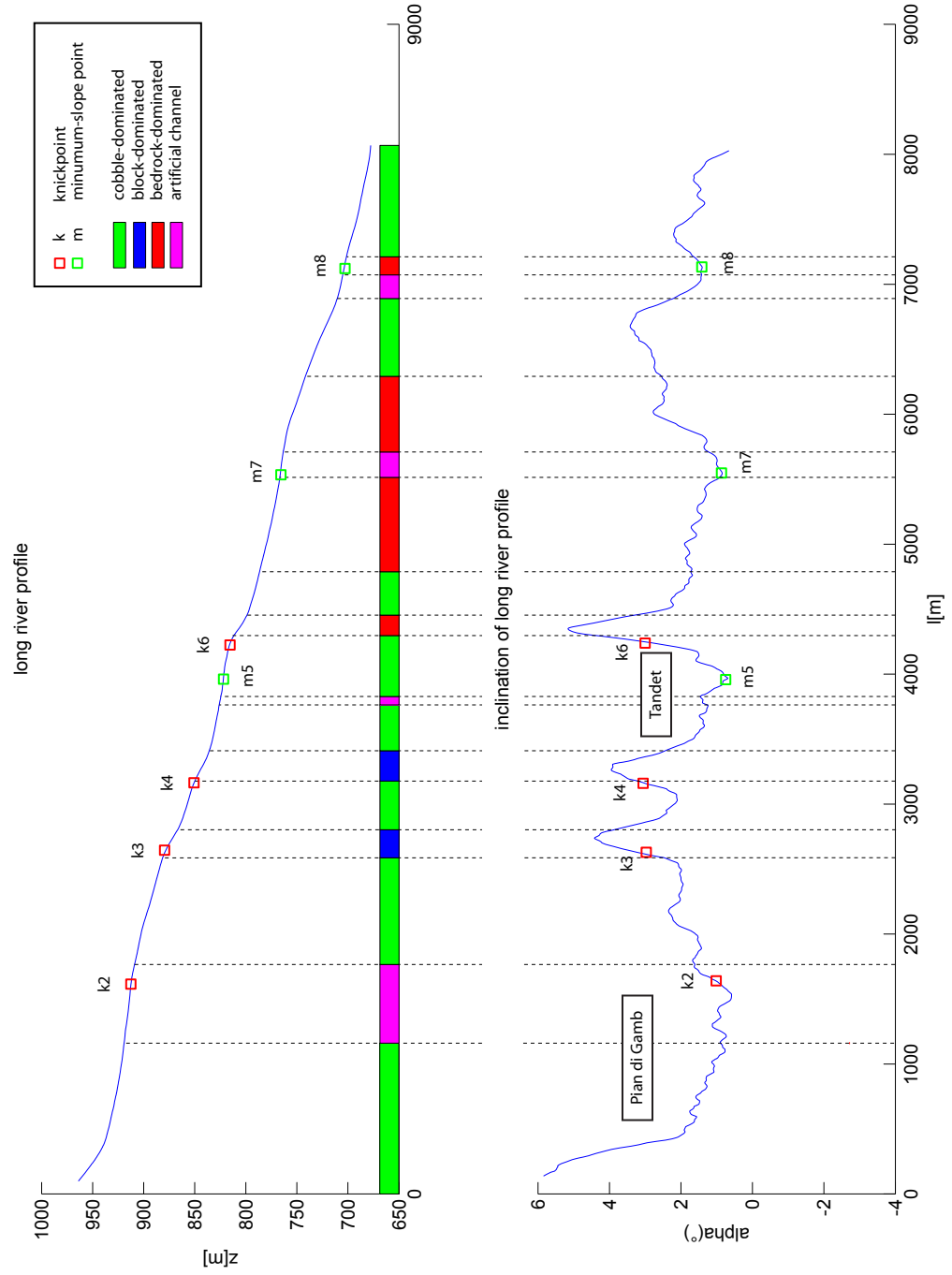


Figure 4.5: long river profile (manual drawing over DTM-AV)

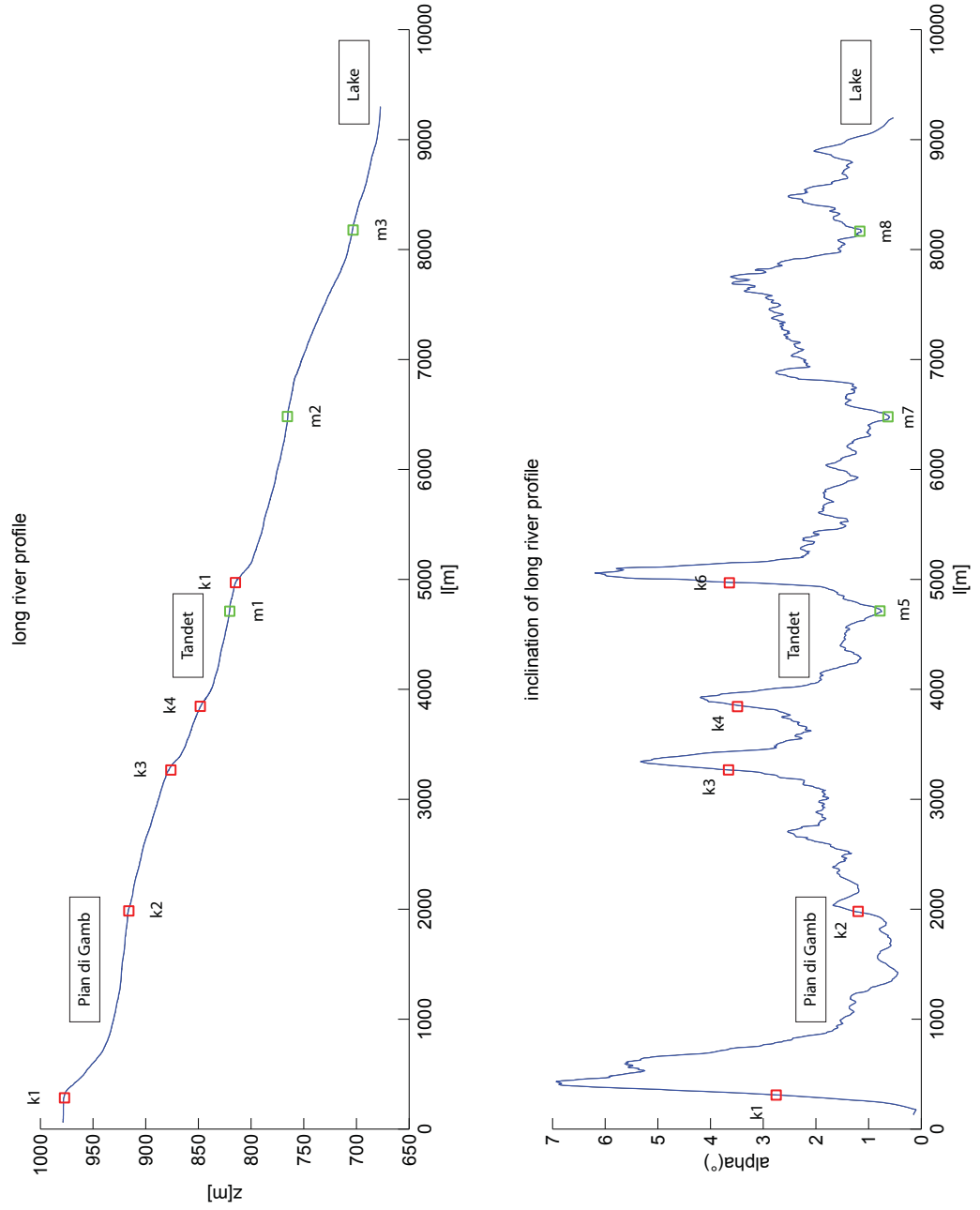


Figure 4.6: long river profile (hydrological accumulations with the DTM-AV)

stretch	class	$a_1[m]$	$a_2[m]$	$b_1[m]$	$a_3[m]$	$b_3[m]$
a	A	25	30	4	80	10
b	B	30	35	3	80	7
c	D	25	35	2	40	4
d	C	5	20	2	30	7
e	D	15	30	4	40	6
f	C	3	10	3	20	6
g	B	20	25	2	F	F

Table 4.2: Means of cross sections's paramenters

4.2 Hydrological results

4.2.1 Periodicity

In a visual analysis, e.g. in a plot of the last four years (see the left plot of Figure 4.7) the signal of the annual streamflow shows a yearly periodicity. Streamflows tend to be larger in the second part of the years than in the first one, which could be due to spring rain and snow melt. During the spring but also during the summer occur the biggest peaks that represent the flood-events. Floods usually last 2-4 days and in the Alps are normally caused by large rainfalls. Also the plot of the amplitudes of the discrete Fourier transformed frequencies shows the same periodicity (see the right plot of Figure 4.7). In this plot there are four peaks: respectively one by frequency 0 (f_1), then by 0.002734 (f_2), 0.005468 (f_3) and 0.008201 (f_4). The peak by the frequency 0 is per definition the mean of the signal. f_2 corresponds to a period of $T = (0.002734 d^{-1})^{-1} = 365.8 d$, which corresponds to the solar year ($365.2 d$). f_3 lies by a frequency that is the double of f_1 , f_4 by a frequency that is three times f_1 . Therefore f_2 must be the fundamental frequency of the signal, while f_3 and f_4 are harmonic frequencies of f_1 .

4.2.2 Empirical streamflow-trend

The probability distribution function (PDF), calculated with the previously described empirical method, shows an exponential decrease toward large streamflows (see Figure 4.8). The cumulative distribution function (CDF) shows an inverse trend, increasing toward large streamflows. Indeed the empirical yearly flood probability (the probability that a streamflow of a certain magnitude happens) does not show a smooth trend, especially for large streamflows. This is due to the rareness of these events that does not allow an empirical analysis. Anyway the plot of the yearly flood probability shows two different trends: in the first part (from 0 to about $60 m^3 s^{-1}$) the probability change rate exponentially increases, but then it starts to asymptotically decrease toward zero. These two trends indicate that there are at least two different streamflow-distributions, the first for the normal streamflows, the second one for the extreme events.

4.2.3 Flood analysis

The analysis of the extreme events has therefore been made using an extreme value distribution. Using the technique of Plotting Position we found that the *Gumbel distribution* (also called *Extreme Value distribution Type I*) fits very well the extreme-event data (see Figure 4.9). Due to this, the return periods have been calculated from probabilities calculated with the Gumbel distribution. Return periods calculated with this

technique have been plotted together with the empirical calculated return period on a semi-logarithmic scale (see Figure 4.9). In spite of the rareness of the extreme events, the empirical calculated curve is not so bad and fits quite good the calculated model.

4.2.4 Sediment motion

In order to understand the reason of the previously described sedimentology, the incipient motion has been calculated for different grain size using (3.8), in particular for the coarsest grains of the granule, pebble and cobble classes. The results are summarised in Table 4.3.

Class	Grain size	Incipient motion [Pa]
granule	4 mm	1670
pebble	6 cm	500
cobble	20 cm	33.4

Table 4.3: Incipient motion for different grain sizes

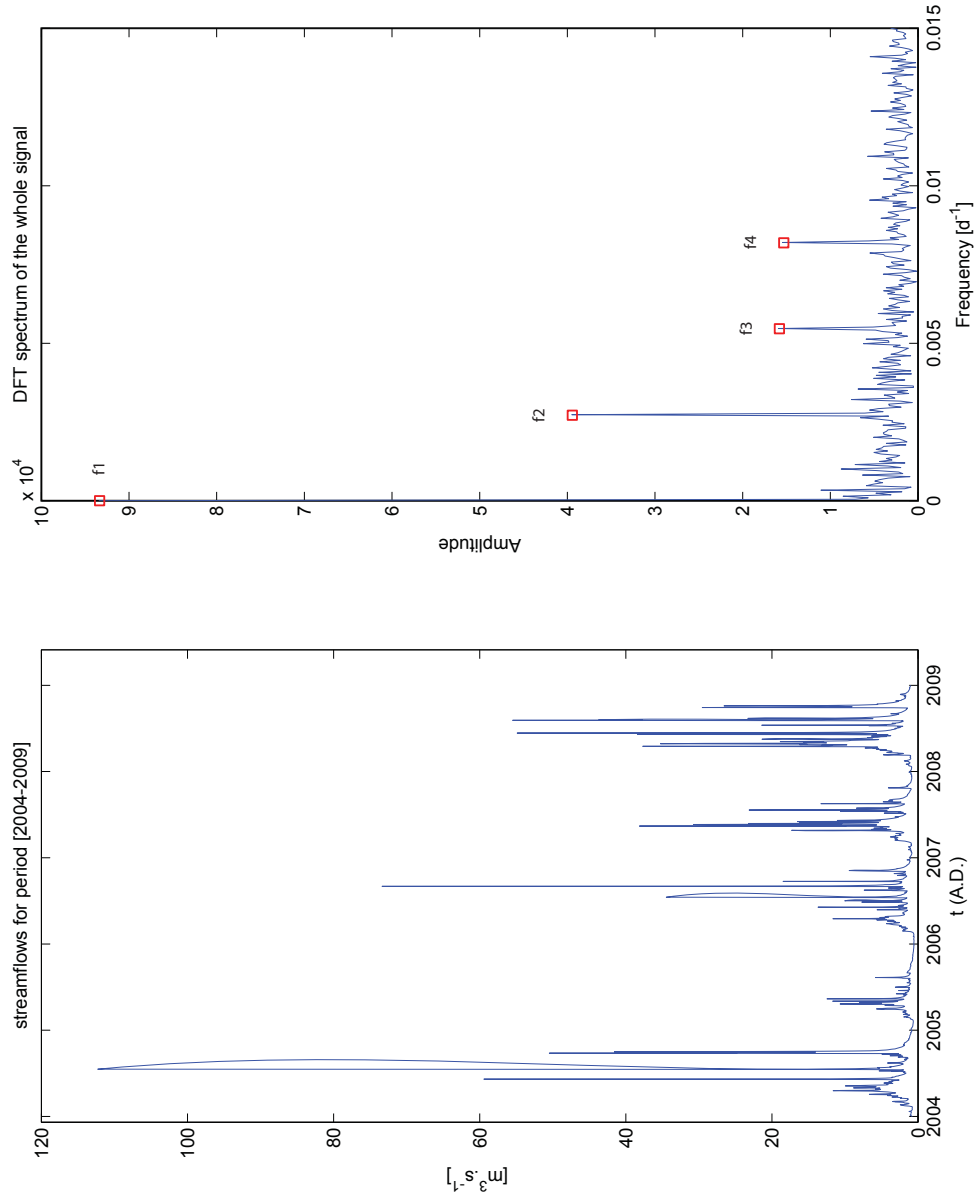


Figure 4.7: Streamflow-periodicity

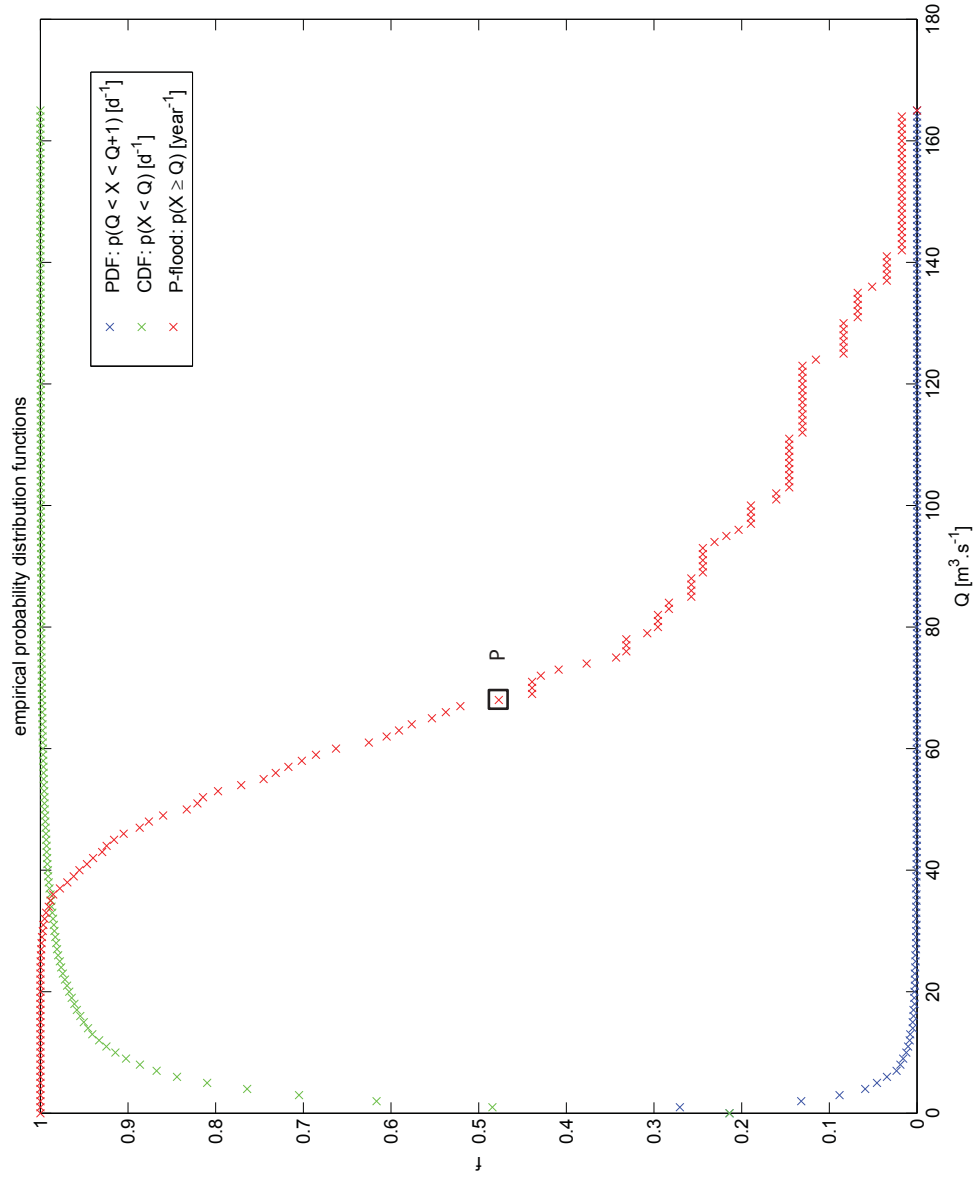


Figure 4.8: Empirical probability distributions

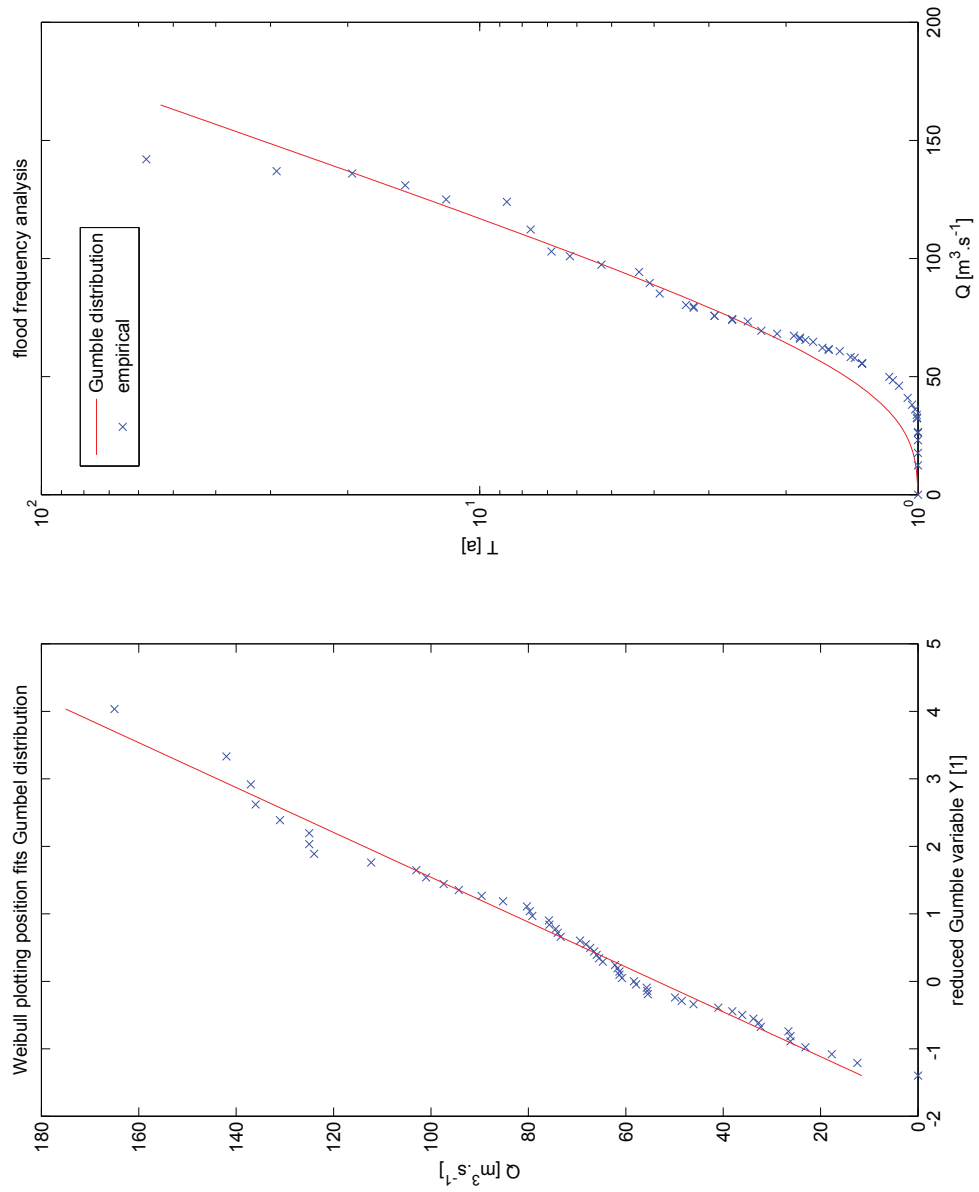


Figure 4.9: Flood analysis

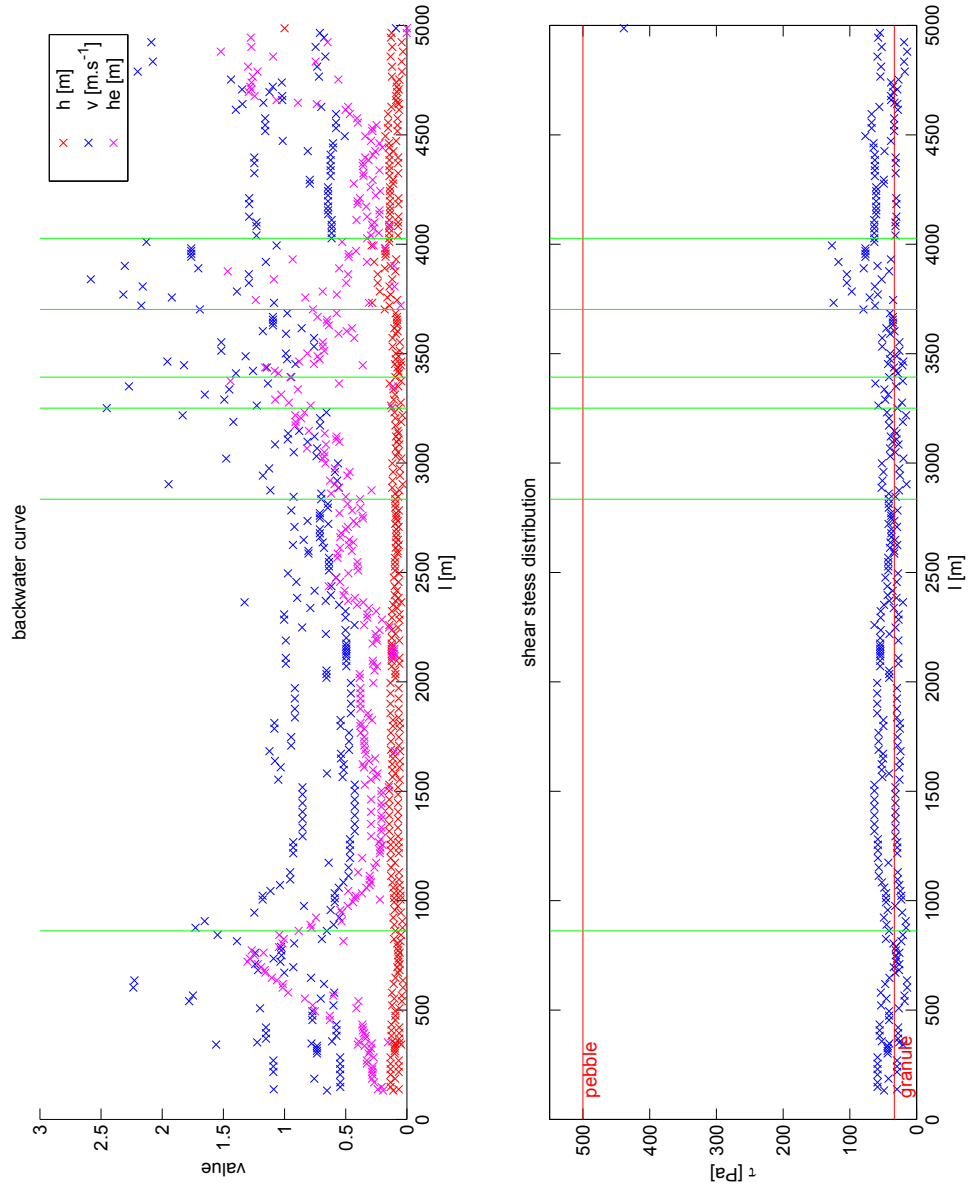
4.2.5 Backwater-curve simulation

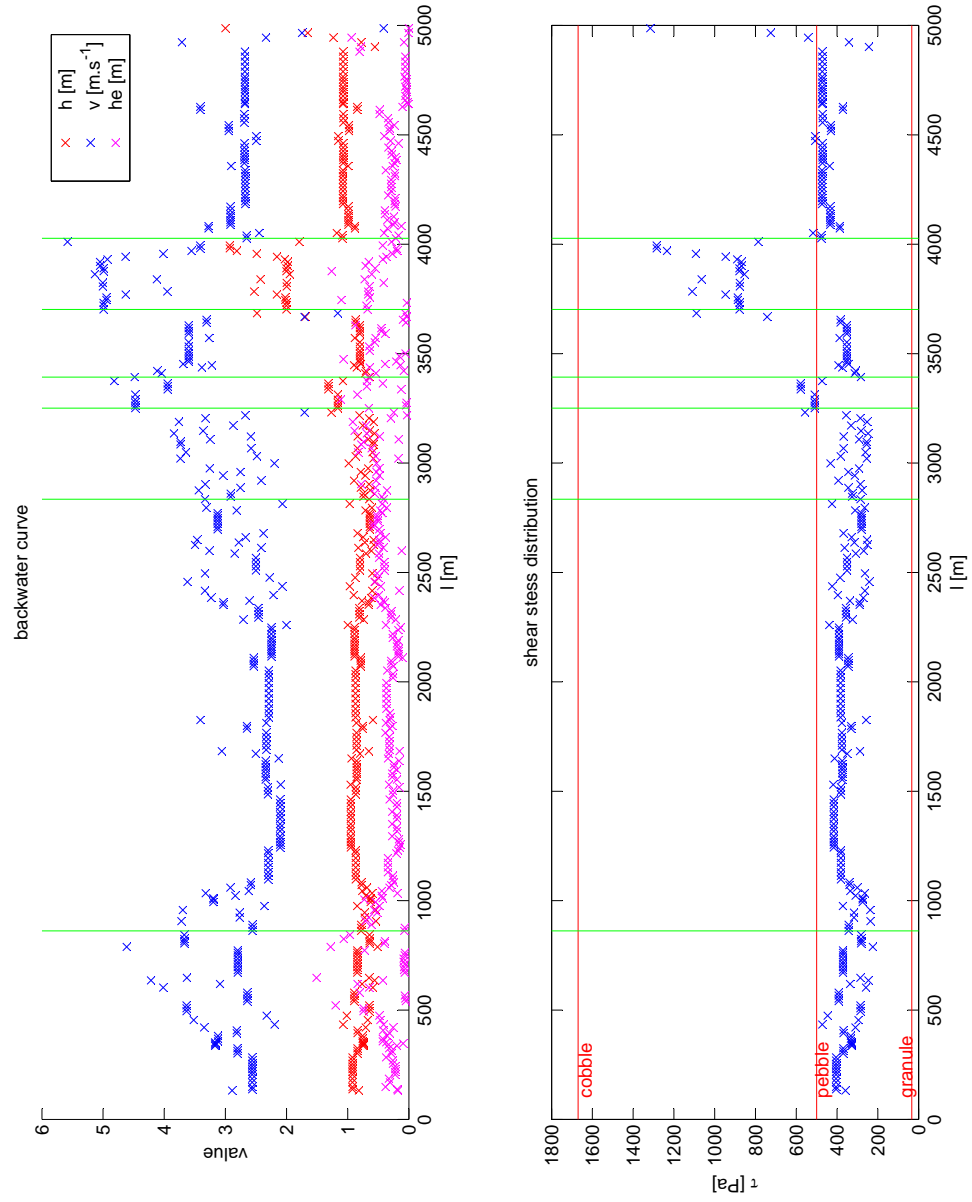
For the calculation of the backwater curve we used a Matlab implementation of the described algorithm. The program has been tested successfully for simple models, such as constant depth but variable cross sections and conversely. In these cases the values calculated from the program converge with the ones predicted from the Manning equation.

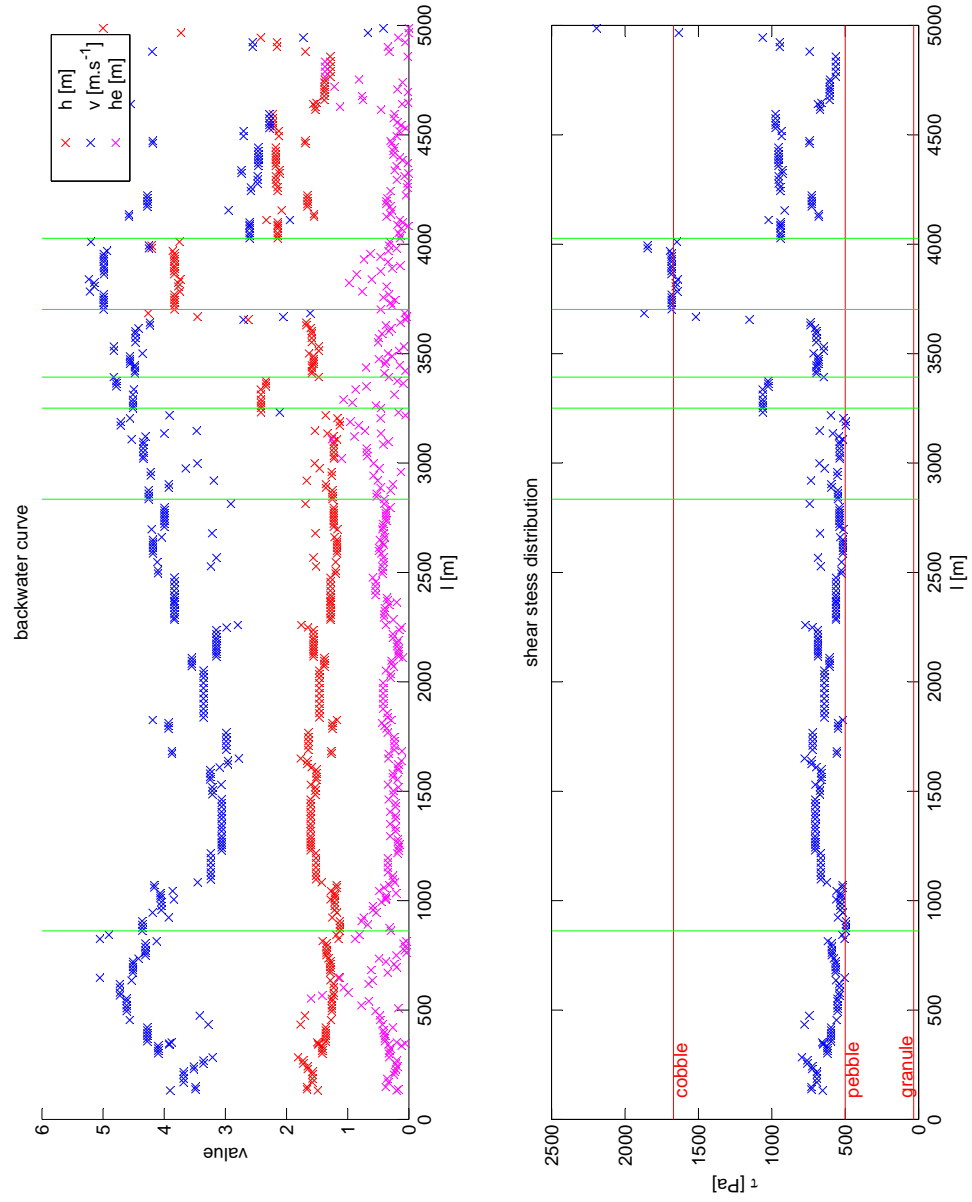
We choosed to use a constant Manning's roughness coefficient for all the cross sections, i.e. 0.05, a typical average value for a mountain river with a gravel bed load. A river simulation has been done for three streamflows: the first one is an every-day flow, the other ones are already flood events of low (2 *a*) respectively medium (11 *a*) return period.

- **Every-day stream** The average of all the streamflow recorded by BAFU is $2.0 \text{ m}^3 \text{ s}^{-1}$, therefore we ran the program with $Q_-=2$ and $h(1,1)=1$. The results are summarized in the plot of Figure 4.10. The river elevation is almost constant over the whole profile by approximately 10 *cm*, with a zone of slight larger values (about 25 *cm*) in stretch *f*. The stream-velocity is mostly by 0.75 m s^{-1} , but in the stretches *a*, *d* and *e* it reaches about 2 m s^{-1} . According to the previously calculated values of shear stress for the sediment incipient motion, in the whole profile the streamflow has enough power to start moving granules and fine pebbles, but *f* the shear stress increases by about 200% and is therefore able to start moving coarser pebbles.
- **2a-flood** According to the previous calculated flood analysis, a flood of $65 \text{ m}^3 \text{ s}^{-1}$ has a return period of 2 *a*. We ran the program with $Q_-=65$ and $h(1,1)=3$ and summarized the results in the plot of Figure 4.11. In this case the water elevation is more variable than in the previous simulation: in most of the profile it is constant by about 1 *m*, but in the stretches *d* and *f* it increases to 1.2 respectively 2 *m*. The velocity is more variable: it is mostly by about 2.5 m s^{-1} , but it increases in *a*, *c* and *e* to approximately 2.5, in *d* to 4.5 and in *f* to 5 m s^{-1} . The results show that such a flood can mobilize pebbles over the whole profile. However, in *d* also fine cobbles can start moving and in *f* also coarser cobbles.
- **11a-flood** A flood of $160 \text{ m}^3 \text{ s}^{-1}$ has an occurrence period of 11 *a*, therefore we ran the program with $Q_-=160$ and $h(1,1)=5$ and we summarized the results in the plot of Figure 4.12. For this flood the variations in the water elevation become more evident: the elevation is mostly by 1.5 *m*, but in *d* it increases to 2.5 and in *f* it rises to 3.5 *m*. The velocity varies also very much: in *a* it is by 4.5 m s^{-1} , then it suddenly decreases to 3 at the begin of *b*, where it begins to constantly increase, reaching 5 m s^{-1} by *f*; in *g* it decreases again to 2.5. Over the whole river profile the river is able to move fine cobbles, but in *d* also coarse cobbles and in *f* it starts moving fine boulders.

In general the shear stress generated by the flood events in the most narrow channels (mostly *f* but also *d*) is always larger than the one genetated in the wide channels and this differences increase for increasing flood magnitudes. However, in section *a*, even if it is the steepest of the studied area, the water elevation never reaches large values, because this section is enough wide to absorb all the energy to increase the flood velocity.

Figure 4.10: Backwater curve simulation with $Q=2$ and $h(1,1) = 1$

Figure 4.11: Backwater curve simulation with $Q=65$ and $h(1,1) = 3$

Figure 4.12: Backwater curve simulation with $Q=160$ and $h(1,1) = 5$

Chapter 5

Interpretations

5.1 Quality of the digital models

The amount of noise in the DTM-AV is larger than we expected. Swisstopo wrote us that the DTM-AV models have been committed to a private company and that they have been made using the LIDAR technology but with lasers optimized for soil-elevation measurements. A water-elevation measurement with LIDAR would be possible but would require additional flights during special conditions, i.e. nadir-flights during calm-water conditions. They also wrote that "the measurements of the water-elevation are more likely randomized and does not correspond to the real elevation of the water". However, after the filtering processes the DTM-AV profiles showed a better resolution than the DTM-25 profiles and it is thank to this higher resolution that we were able to analyse in detail the knickpoints of a shorter part of the profile.

5.2 First interpretation

The block-dominated rockslides of Isolan, Gagna della Scranna and Miaddi happened a long time ago. The material of one or of all of them obstructed the valley and formed a small lake, in a way similar to Korup's description [Korup, 2005]. This interpretation is supported by the following arguments:

- **History** In historical registers a lake at the place of the present Piano di Alne (northern of Cauco) has been documented by Bertossa [Bertossa, 1937]. Its origin has been the consequence of the obstruction of the valley with the material of *Campo-Bagigno*'s landslide, which took place the 30th September 1513. This landslide happened in the same day of the famous landslide that formed the *Buzza di Biasca*-dam at the end of the Blenio valley [Pometta, 1932]. However, the dating of the disappearance of the lake over Cauco is still debated within the interval from 1536 to 1672. On my opinion the XVI century could be more realistic, because also Biasca's lake collapsed in 1515 flooding the small city of Biasca and the whole Magadino's plane [Various, 1992]. Unfortunately, we did not have enough time to better search for a core of the material of the Pian di Gamb alluvial plane: the presence of limno-sediments would be the ultimate proof of the existence of this second paleolake.
- **Morphology** The block-dominated channel corresponds to the rockslide-area of Isolan, Gagna della Scranna and Miaddi. This blocks cover both sides of the

valley, where there is no concrete erosion. This means that the rockslide itself was already block-dominated.

- **Long river profile** At the end of the large alluvial plane of Pian di Gamb the inclination increases, reaches a maximum by the block-dominated channels and then decreases again by the alluvial plane of Tandet. Pian di Gamb could be more flat because of the sedimentation in the basin created by the dam, the block-dominated zone could be steeper because of the incision in the material deposited by the rockslide.
- **Sedimentology** The sedimentology of the river bed changes from cobble-dominated to block-dominated. This is probably due to a change in the river's erosion-potential, but also to the material deposited by the block-dominated rockslide.
- **Hydrology** The hydrological simulation has been runned with actual parameters and can therefore only explain actual erosion processes. From the backwater-curve simulations we can deduce the following statements.
 - Granules can always be mobilized along the whole river profile, which corresponds to the observation that all the channels lack in the granule and sand fractions.
 - In the wide channels of the alluvial planes, e.g. in Pian di Gamb, fine pebbles can be mobilized by a common flood ($T = 2 a$, $Q = 65 m^3 s^{-1}$) but coarser pebbles require a larger and rarer one ($T = 11 a$, $Q = 160 m^3 s^{-1}$). This corresponds to the actual sedimentation, because the channels of the alluvial planes are pebble-dominated.
 - In the most narrow channel the common flood of $65 m^3 s^{-1}$ is able to start moving coarse cobbles and the rarer flood of $160 m^3 s^{-1}$ is able to start moving also fine boulders. During the floods this stretch is subjected to both the largest shear stress and the largest flow-velocities. Therefore it could be hypothesized that during the floods large quantities of clasts, i.e. granule, pebbles and cobbles, have been transported downstream. As we always calculated the incipient motion, we only can say which sediments can be mobilized, without opining if the river is able to transport them downstream. However, the fact that the river is able to move sediments up to fine boulders supports the hypothesis that a part of the fine sediments could have been transported downstream.

5.3 Second interpretation

The second interpretation is that the three landslides of Isolan, Gagna della Scranna and Miaddi never fully obstructed the river. The alluvial plane of Pian di Gamb could have been filled with the material generated by the rupture of the dam created by *Campo-Bagigno's* landslide. However, this second interpretation does not modify the previous discussion: even though the three block-dominated landslides were smaller, they would also have modified the river dynamics, i.e. increasing the Manning's roughness coefficient, which would slow the river down and increase the shear stress. This would cause the incision of the narrow channel. However, this interpretation does not explain the origin of the alluvial plain of Tandet, which origin could probably be connected with the beginning of the detachment-limited channel by Arvigo.

Chapter 6

Conclusions

6.1 Summary

This study focuses on a short part of the river of the Calanca Valley, southern Switzerland. The combination of field work and analyses of digital models and streamflow measurements allowed us to research on the sedimentology of the river bed, the geomorphology of the valley's sides, the long river profile, the cross-sections and the return period of the extreme streamflows. The results of these different analysis are well correlated. In particular we discovered that the three block-dominated landslides between Selma and Arvigo have influenced the river sedimentation. This resulted in a change in the shapes of the long river profile and of the cross sections. Actually, this last two parameters still influence the river dynamics. Especially during flood events in this channel the shear stress is able to mobilize sediments up to cobbles, which in the field results in a lack of fine sediments.

6.2 Future work

This study is only a first general study of the river between Cauco and Buseno. To better understand all the correlations and to prove if one of the our interpretations is true additional studies are needed and we recommend to undertake the followings investigations:

- Detailed geomorphological mapping, comparing the DTM-AV stuctures with air-photos and field observations.
- Study of the origin of the knickpoint by Arvigo, where the channel changes from be transport-limited to be detachment-limited.
- Numerical-simulation with precise DTM-AV cross-section- and long river profile-data of the ability of the river to transport downstream sediments of different grain-sizes.

6.3 Acknowledges and thanks

Acknowledges goe to Dr. Peter Molnar for its precious teaching and its supervision about the river hydrology and to Dr. Andrew Kos for its supervision of the geological part of the study. I also thank Freddy X. Yugsi Molina for its teaching about the Geographic Information System ArcGIS, Kerry Leith for the precious review of the draft of this work, my father Michele Guglielmetti for the review of the probability calculations and my sister Sonia Guglielmetti for the English corrections.

I miei piu' sentiti ringraziamenti ai camionisti della val Calanca per gli strappi fitti di rilassante chiacchiericcio, alla barista che mi offriva sempre il caffè' e all'anziano signore che mi ha salvato da famelici deliri regalandomi ben due pagnotte di segale appena sfornate.

Bibliography

- [Abele, 1974] Abele, G. (1974). *Bergstuerze in den Alpen ihre Verbreitung, Morphologie und Folgeerscheinungen: Wissenschaftliche Alpenvereinshefte*. Deutscher und Oesterreichischer Alpenverein, Muenchen.
- [Berger et al., 2007] Berger, A., Mercolli, I., and Engi, M. (2007). *Tectonic and Petrographic Map of the Central Lepontine Alps, 1:100000*. Federal office of topography Swisstopo, Bern.
- [Bertossa, 1937] Bertossa, A. (1937). *Storia della Calanca*. Tipografia fu F.Menghini, Poschiavo.
- [Blair and McPherson, 1999] Blair, T. C. and McPherson, J. G. (1999). Grain-size and textural classification of coarse sedimentary particles. *Journal of Sedimentary Research*, 69:6–19.
- [Eisbacher and Clague, 1984] Eisbacher, G. H. and Clague, J. J. (1984). Destructive mass movements in high mountains. *Geological Survey of Canada Paper*, 84(16):19–21.
- [Fossati, 2008] Fossati, D. (2008). *The deep seated gravitational slope deformation of Landarenca (Graubunden, Switzerland)*. Unpublished ETH Zurich Master thesis, Zuerich.
- [Gumbel, 1958] Gumbel, E. J. (1958). *Statistics of Extremes*. Columbia University Press, New York.
- [Korup, 2005] Korup, O. (2005). Large landslides and their effect on sediment flux in south westland, new zealand. *Earth Surface Process and Landforms*, 30:305–307, 320.
- [Korup and Schlunegger, 2007] Korup, O. and Schlunegger, F. (2007). Badrock land-sliding, river incision and transience of geomorphic hillslope-channel coupling: evidence from inner gorges in the swiss alps. *Journal of geophysical research*, 112:1–3.
- [Maidment, 1993] Maidment, D. R. (1993). *Handbook of Hydrology*. McGraw-Hill, New York.
- [Matula, 1981] Matula, M. (1981). Rock and soil description and classification for engineering geological mapping report by the iaeg commission on engineering geological mapping. *Bulletin of Engineering Geology and the Environment*, 24:235–274.
- [Pometta, 1932] Pometta, E. (1932). La buzza di biasca e le sue conseguenze. *Bollettino storico della Svizzera Italiana*, pages 105–109.

- [Seiffert, 1960] Seiffert, R. (1960). *Zur Geomorphologie des Calancatales*. Geographisch-Ethnologischen Gesellschaft Basel, Basel.
- [Shields, 1936] Shields, A. (1936). *Anwendung der Aehnlichkeitsmechanik und der Turbulenz Forschung auf die Geschiebebewegung*. Preussische Versuchsanstalt fuer Wasserbau und Schiffbau, Berlin.
- [Tucker and Whipple, 2002] Tucker, G. E. and Whipple, K. X. (2002). Topographic outcomes predicted by stream erosion models: Sensitivity analysis and intermodel comparison. *Journal of Geophysical Research*, 107.
- [Various, 1992] Various (1931-1992). *Atti concernenti la Buzza di Biasca*. Archivio di Stato del Canton Ticino, Bellinzona.
- [Various, 2008] Various (2008). *HEC-RAS Hydraulic Reference Manual*. U.S. Army Corps of Engineers, Davis.

Appendix A

Additional data

A.1 Additional tables

Section		Cross section parameters				
ID	Stectch	b1 [m]	b2 [m]	a1 [m]	b3 [m]	a2 [m]
1	a	29.5	32.0	5.0	54.0	6.0
2	a	20.0	30.0	3.0	100.0	14.0
3	b	55.0	40.0	4.5	95.0	10.0
4	b	19.0	28.0	4.0	160.0	4.0
5	b	32.5	39.5	2.0	24.0	10.0
6	b	22.0	27.0	1.7	34.0	7.0
7	c	37.0	48.0	2.0	55.0	3.5
8	c	16.0	28.0	1.5	32.0	4.0
9	c	16.0	26.0	2.0	38.0	5.0
10	d	6.0	21.0	1.5	29.0	7.0
11	e	16.0	28.0	3.5	42.0	6.0
12	f	3.0	10.0	3.0	22.0	6.0
13	g	23	25.0	2.0		
14	g	13.0	25	3.0		
15	g	22.0	24.0	2.0		

Table A.1: Measured cross section parameters

A.2 Additional maps

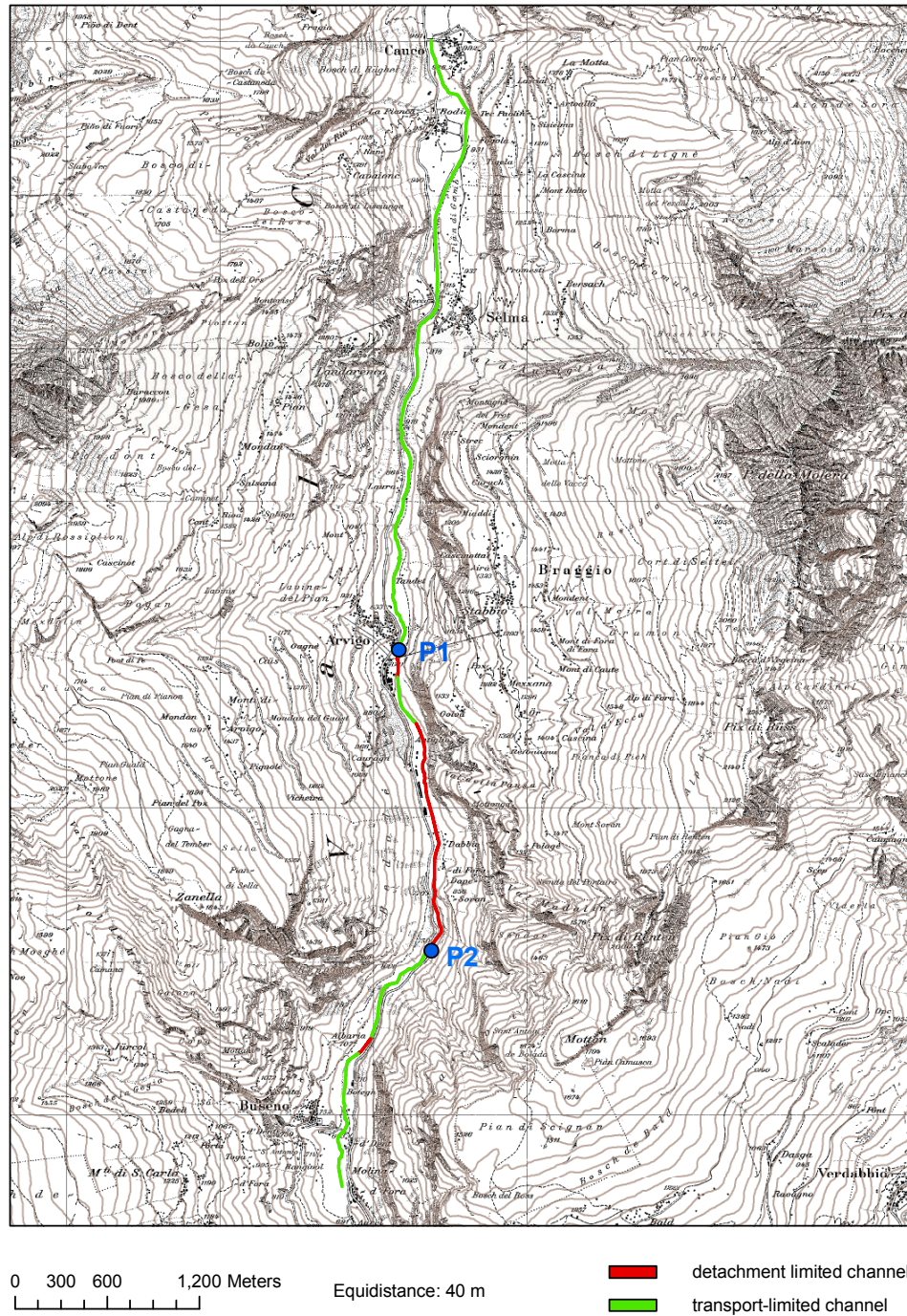


Figure A.1: An overview of the dynamics of the river erosion in the study area

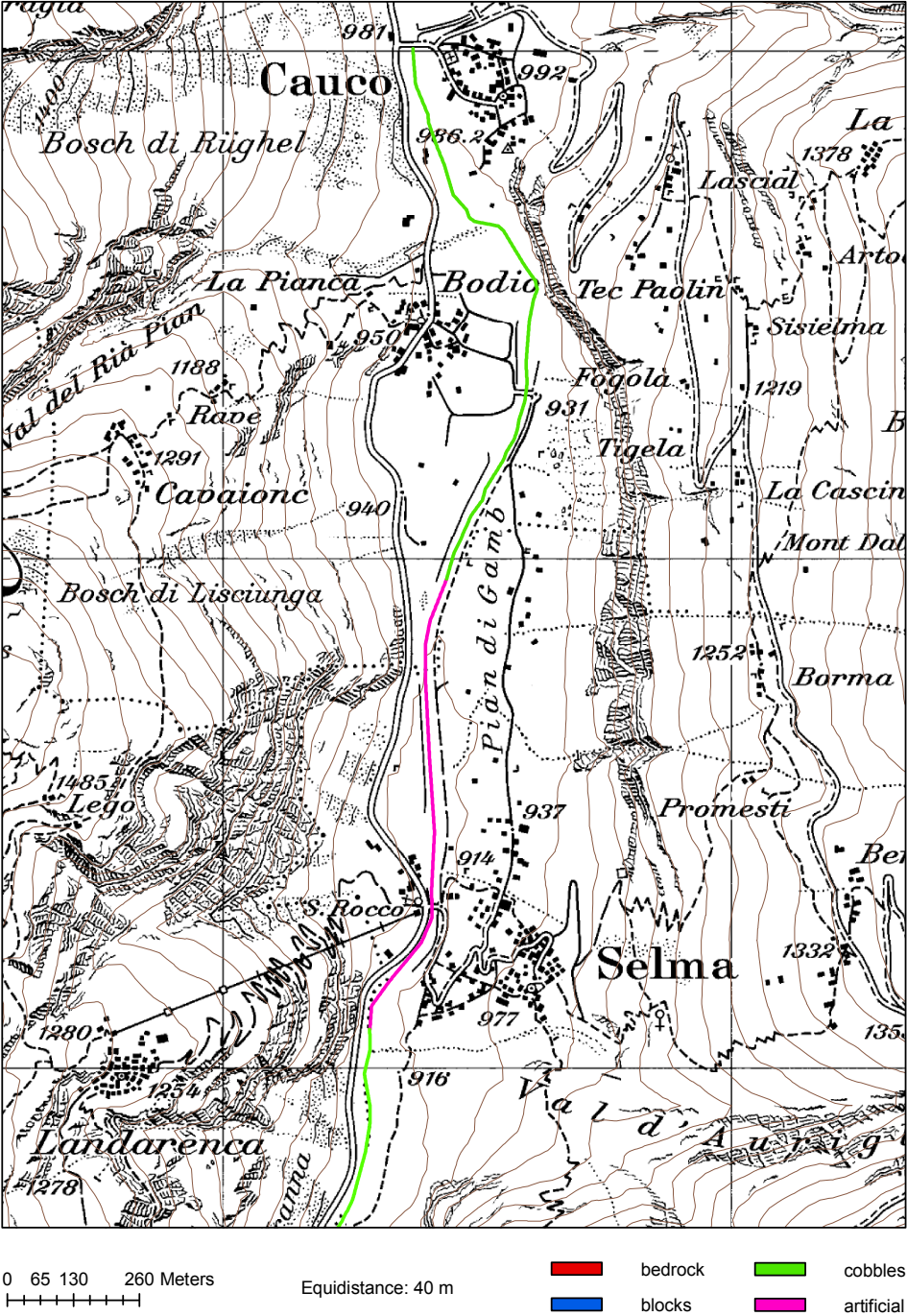


Figure A.2: Sediment map of the northern part of the study area

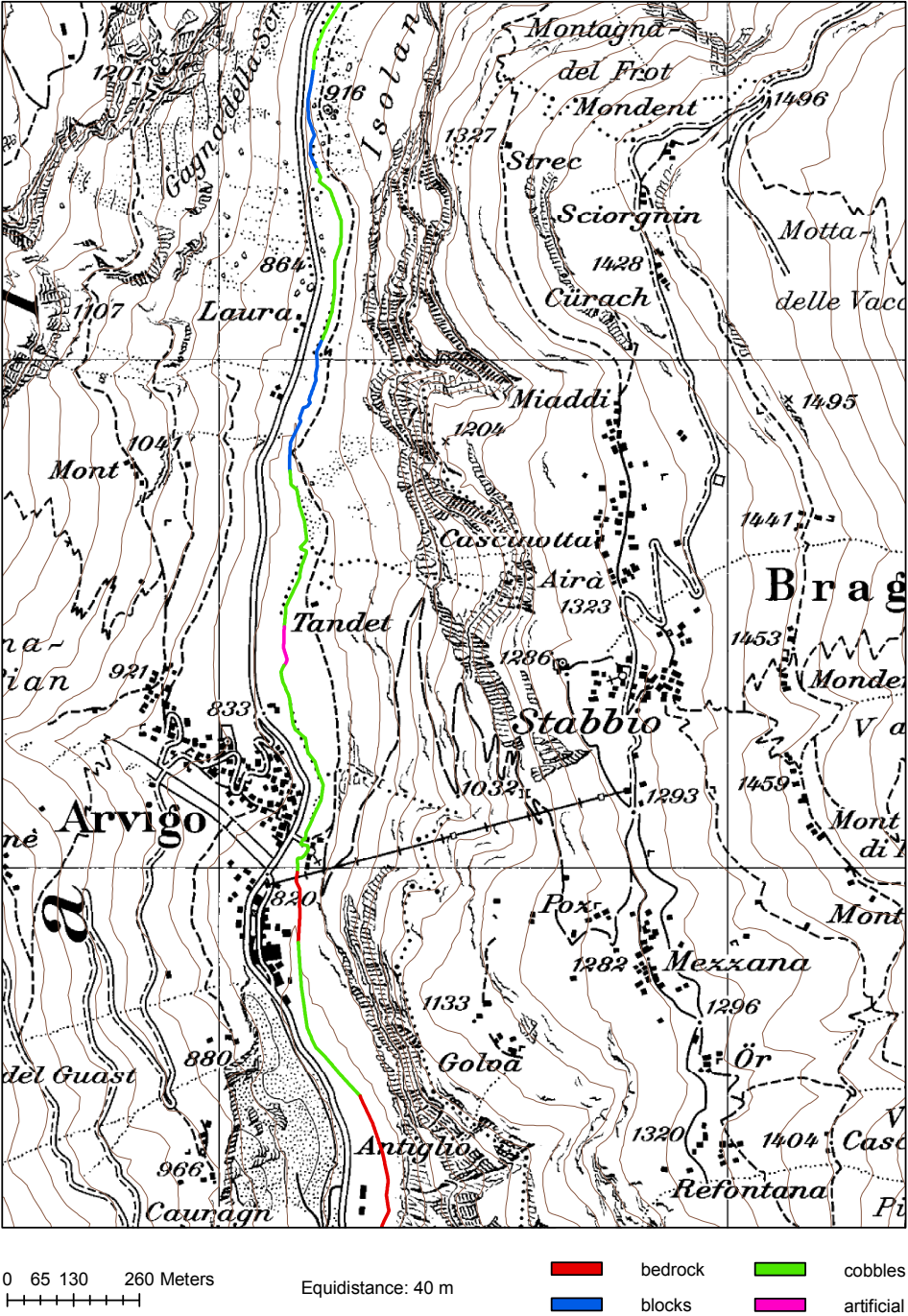


Figure A.3: Setiment map of the central part of the study area

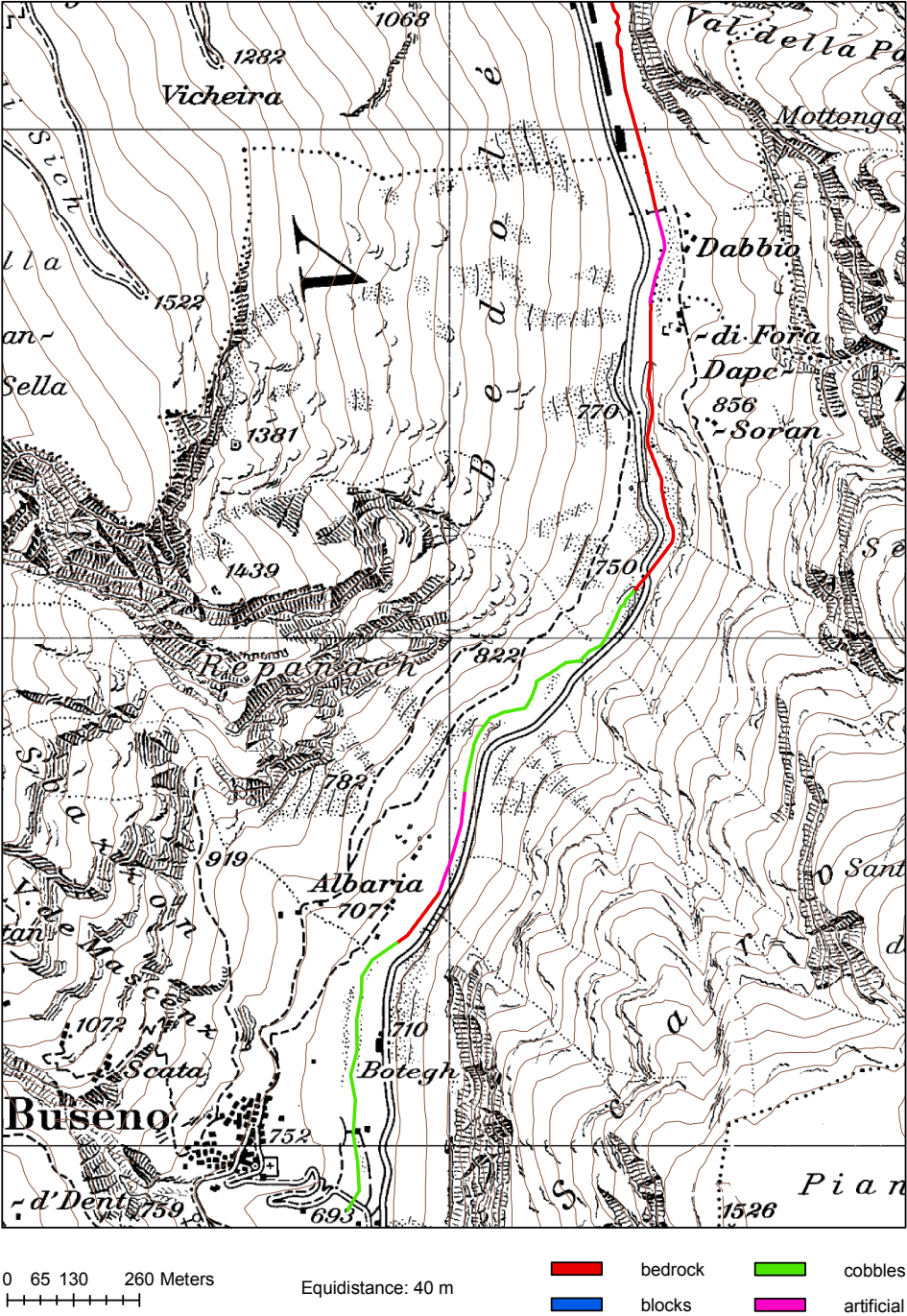


Figure A.4: Sediment map of the southern part of the study area

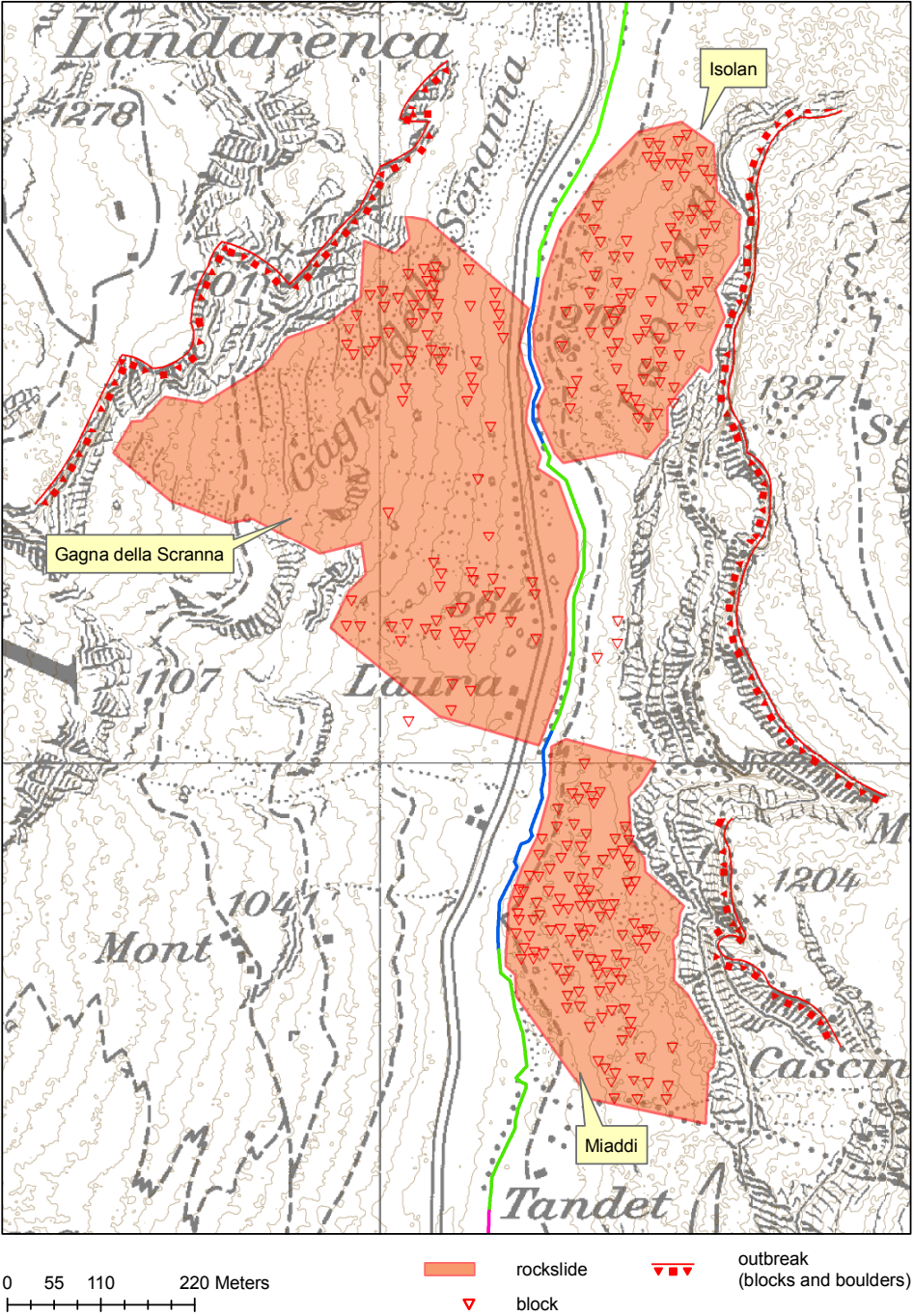


Figure A.5: Morphological map

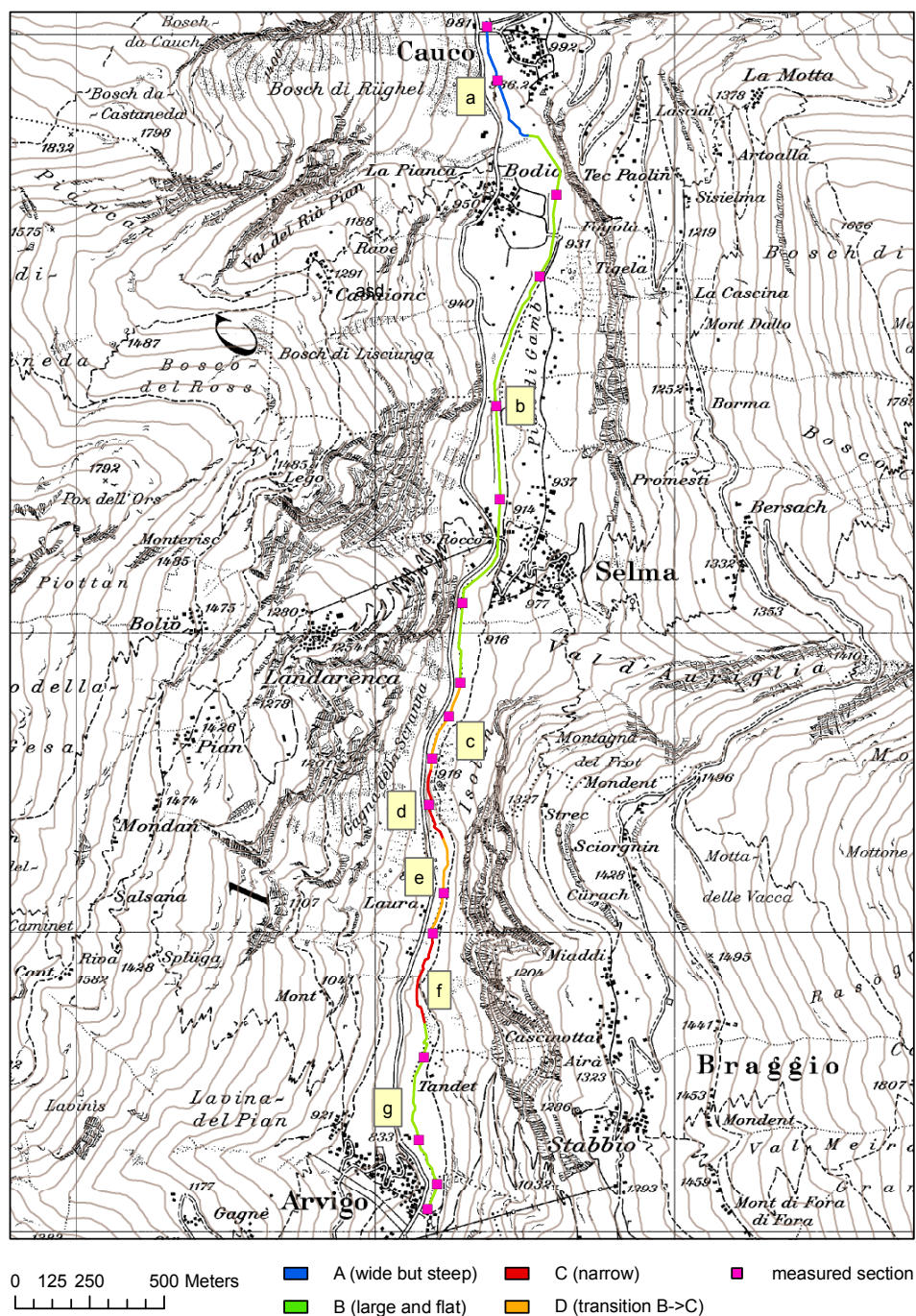


Figure A.6: Cross section classification

Appendix B

Source codes

B.1 Backwater curve simulation

The program for the backwater curve simulation has been written for Matlab. This code is also available at the following URL:

<http://n.ethz.ch/~lucagu/pub/bachelor-thesis/river-simulation/>

B.1.1 main.m

```
clear;

% loading of the data
data = load('dtm_25_cal.txt');

l = flipud(data(:,1));      % length
z = flipud(data(:,2));      % elevation

% cross section parameters
b1 = flipud(data(:,3));
b2 = flipud(data(:,4));
h1 = flipud(data(:,5));
b3 = flipud(data(:,6));
h2 = flipud(data(:,7));

n_manning = flipud(data(:,8));
changepoint = flipud(data(:,9));

% constants
N_ = length(l);             % # sections
I_ = 20;                    % max iterations
ERROR_TOLERANCE_ = 0.1;     % max error in the guess [m]

% variables
n = 0;                      % current cross section iteration
i = 0;                      % current h-iteration

% temp values needed by the algorithm
```

```

h = zeros(N_,I_);           % estimated wassersaeule
h_c = zeros(N_,I_);         % calculated wassersaeule
err = zeros(N_,I_);         % errors of estimated velocities

% temp values that can be overwritten
vv = zeros(I_,1);           % temp v
KK = zeros(I_,1);           % temp K
tmp_x = 0;                   % a result of a query
tmp_i = 0;                   % the index of the result of a query

% definitive values
A = zeros(N_,1);             % cross section's area
p = zeros(N_,1);             % cross section's perimeter
h_t = zeros(N_,1);           % theoretical river height
v_t = zeros(N_,1);           % theoretical flow velocity
hdef = zeros(N_,1);          % good values of wassersaeule
he = zeros(N_,1);            % energy loss
v = zeros(N_,1);             % flow velocities
K = zeros(N_,1);             % channel conveyance factor
sfm = zeros(N_,1);           % middle friction slope
sc = zeros(N_,1);            % river-channel slope
tau = zeros(N_,1);           % shear stress
error = zeros(N_,1);         % section where the algorithm does not converge

% physical constants
g_ = 9.81;                   % gravitational acceleration
rho_ = 1000;                 % density of the fluid
ip_ = [33.3;500;1670];       % incipient motion for some classes of grain size
ip_label_ = strvcat('granule','pebble','cobble');

% BOUNARY CONDITIONS
Q_ = 160;                    % streamflow
h(1,1) = 5;                  % water elevation at the start point

% calculations for the startpoint
A(1) = get_area(b1(1),b2(1),h1(1),b3(1),h2(1),h(1,1));
p(1) = get_perimeter(b1(1),b2(1),h1(1),b3(1),h2(1),h(1,1));
K(1) = 1 / n_manning(1) * A(1) * (A(1) / p(1) )^(2/3);
v(1) = Q_/A(1);
hdef(1) = h(1,1);

for n=2:N_
    i = 0;
    while i <= I_-1
        i = i + 1;

        switch i
            % estimation ot the water depth
            case {1}; h(n,i) = hdef(n-1);

```

```

case {2}; h(n,i) = h(n,i-1) + 0.7*err(n,i-1);
otherwise;
    err_diff = h(n,i-1) - h_c(n,i-1) + err(n,i-2);
    if (abs(err_diff) >= 0.01);
        h(n,i) = h(n,i-2) - err(n,i-2)*( h(n,i-2) - h(n,i-1) )
            /(err_diff);
    else
        h(n,i) = (h(n,i-1) + h_c(n,i-1)) / 2;
    end
end

if( i > 1 )
    % limitation of the changerate
    change_rate = h(n,i) / h(n,i-1);
    if ( change_rate < 0.5 )
        h(n,i) = 0.5 * h(n,i-1);
    elseif ( change_rate > 2 )
        h(n,i) = 2 * h(n,i-1);
    end
end

% limitation of the water elevation below the channel
if( h(n,i) > h2(n) )
    h(n,i) = h2(n);
end

% area and wetted perimeter
A(n) = get_area(b1(n),b2(n),h1(n),b3(n),h2(n),h(n,i));
p(n) = get_perimeter(b1(n),b2(n),h1(n),b3(n),h2(n),h(n,i));

% theoretical values
sc(n) = (z(n)-z(n-1))/(l(n-1)-l(n));
h_t(n) = ( (n_manning(n) * Q_)/(sqrt(sc(n))*b2(n)) )^(3/5);
v_t(n) = 1 / n_manning(n) * ( (h_t(n)*b2(n))/(b2(n)+2*h_t(n)) )^(2/3)
    *sqrt(sc(n));

% calculate friction generated by the estimated depth
KK(i) = A(n) / n_manning(n) * (A(n) / p(n))^(2/3);
vv(i) = Q_ / A(n);

sfm(n) = (2*Q_ / (K(n-1) + KK(i)))^2;
he(n) = (l(n-1)-l(n)) * sfm(n);

% real water depth generated with energy balance
h_c(n,i) = z(n-1) - z(n) + ( v(n-1)^2 - vv(i)^2)/(2*g_) + hdef(n-1)
    + he(n);

% checkpoint
err(n,i) = h_c(n,i) - h(n,i);

```

```

sprintf('%i,%i; h=%c err=%c', n, i, h(n,i), err(n,i));

if(abs(err(n,i)) <= ERROR_TOLERANCE_ )
    hdef(n) = h(n,i);
    v(n) = vv(i);
    K(n) = KK(i);
    break;
end
end

% in the case that the algorithm does not converge
if( i == I_ )
    if ( hdef(n) == 0 )
        [tmp_x, tmp_i] = min( abs(err(n,:)) );
        hdef(n) = h(n, tmp_i);
        v(n) = vv(tmp_i);
        K(n) = KK(tmp_i);
        error(n) = 1;
    else
        sprintf('nothing is impossible..')
        return;
    end
end
end

% shear stress
tau = rho_.*g_.*hdef.*sc(n);

figure(1);
clf;

subplot(2,1,1);
hold on;
plot(l,hdef,'xr');
plot(l,v,'xb');
plot(l,he,'xm');
xlabel('l [m]'); ylabel('value'); title('backwater curve');
legend('h [m]', 'v [m.s^{-1}]', 'he [m]');
hold off;

for n=1:N_
    if(changepoint(n) == 1)
        vline(l(n),'-g');
    end
end

subplot(2,1,2);
plot(l,tau,'x');
xlabel('l [m]'); ylabel('\tau [Pa]'); title('shear stress distribution');

```

```

for n=1:length(ip_)
    ip_(n);
    hline(ip_(n),'-r',ip_label_(n,:));
end

for n=1:N_
    if(changepoint(n) == 1)
        vline(l(n),'-g');
    end
end
end

```

B.1.2 get_area.m

```

function A=get_area(b1,b2,h1,b3,h2,h)

    if (h <= h1)
        A = (b1+b2)*h/2;
    elseif (h <= h2)
        A = (b1+b2)*h1/2 + (b2+b3)*(h-h1)/2;
    else
        sprintf('flood')
        return;
    end

end

```

B.1.3 get_perimeter.m

```

function p = get_perimeter(b1,b2,h1,b3,h2,h)

    if (h <= h1)
        alpha = atan( h1 / ((b2-b1)/2) );
        p = b1 + 2*h/sin(alpha);
    elseif (h <= h2)
        alpha1 = atan( h1 / ((b2-b1)/2) );
        alpha2 = atan( (h2-h1) / ((b3-b2)/2) );
        p = b1 + 2*h1/sin(alpha1) + 2*(h-h1)/sin(alpha2);
    else
        sprintf('flood')
        return;
    end

end
end

```

B.2 Additional codes

B.2.1 Smaller Matlab programs

Smaller Matlab programs have been also written to analyse the streamflow data and to smooth the long river profile. They can be downloaded at the following URLs:

<http://n.ethz.ch/~lucagu/pub/bachelor-thesis/stream-analysis/>

<http://n.ethz.ch/~lucagu/pub/bachelor-thesis/profiles/>

B.2.2 \LaTeX source files

This study has been written in \LaTeX . The source files are available at the following URL:

<http://n.ethz.ch/~lucagu/pub/bachelor-thesis/tex/>